

In presenting the dissertation as a partial fulfillment of the requirements for an advanced degree from the Georgia Institute of Technology, I agree that the Library of the Institution shall make it available for inspection and circulation in accordance with its regulations governing material of this type. I agree that permission to copy from, or to publish from, this dissertation may be granted by the professor under whose direction it was written, or in his absence, by the Dean of the Graduate Division when such copying or publication is solely for scholarly purposes and does not involve potential financial gains. It is understood that any copying from, or publication of, this dissertation which involves potential financial gain will not be allowed without written permission.

Paul Louis Goodfriend

THE MAGNETIC ROTATION SPECTRUM
OF NITROGEN DIOXIDE

A THESIS

Presented to
the Faculty of the Graduate Division
Georgia Institute of Technology

In Partial Fulfillment
of the Requirements for the Degree
Doctor of Philosophy in the School
of Chemistry

By
Paul Louis Goodfriend
March 1957

58
12C

THE MAGNETIC ROTATION SPECTRUM
OF NITROGEN DIOXIDE

Approved:

[Handwritten signature]

[Handwritten signature]

[Handwritten signature]

Date Approved by Chairman: March 8, 1957

ACKNOWLEDGMENTS

I wish to thank Professor W. H. Eberhardt not only for suggesting this problem, but also for the guidance he has given me and the patience he has shown in its execution. I am grateful to Dr. J. K. Gladden and Dr. T. L. Weatherly for reading the manuscript and offering valuable suggestions. I also wish to express my gratitude to the Research Corporation for a fellowship for the summer of 1953, to the Graduate School of Georgia Institute of Technology for a fellowship for the 1954-55 academic year, and to the National Science Foundation for a fellowship from June, 1955 to June, 1956. I wish to thank my wife, Beverly, for typing the entire thesis and for being a friend as well as a wife.

TABLE OF CONTENTS

	Page
ACKNOWLEDGMENTS	ii
LIST OF TABLES.	iv
LIST OF ILLUSTRATIONS	v
ABSTRACT.	vi
Chapter	
I. INTRODUCTION	1
II. REVIEW OF LITERATURE	5
III. THEORETICAL CONSIDERATIONS	15
IV. APPARATUS AND CALIBRATION.	22
V. DESCRIPTION OF EXPERIMENTS	31
VI. RESULTS AND DISCUSSION	35
VII. CONCLUSIONS AND RECOMMENDATIONS.	74
Appendices	
I. ZEEMAN EFFECT IN A LINEAR TRIATOMIC MOLECULE WITH VIBRATIONAL ANGULAR MOMENTUM AND THE INTENSITY DISTRIBUTION IN THE MAGNETIC ROTATION SPECTRUM.	78
II. POLARIZATION OF TRANSITION MOMENT.	80
III. OTHER POSSIBLE ASSIGNMENTS FOR THE TRANSITION.	82
IV. SAMPLE CALCULATION OF g AND $(A''-B'')$	84
V. THERMODYNAMIC CALCULATIONS AND THE PREDISSOCIATION LIMIT.	86
VI. TABLES.	88
VII. MICROPHOTOMETER TRACE OF THE MAGNETIC ROTATION SPECTRUM OF NO_2 FROM 6760 Å TO 5200 Å.	93
BIBLIOGRAPHY.	98
VITA.	102

LIST OF TABLES

Table	Page
1. Vibrational Constants for NO_2	11
2. Rotational Constants for NO_2	11
3. Quantum Numbers for Allowed Transitions.	48
4. Number and Characterizations of Sub-bands for Various Values of V_2'	50
5. Wave-lengths and Frequencies of Features in the 7410 A Band	54
6. Wave Number Differences Between Features in the 7410 A Band	55
7. Wave-lengths and Frequencies of Features in the 6720 A Band	62
8. Wave Number Differences Between Features in the 6720 A Band	63
9. Wave-lengths and Frequencies of Features in the 7090 A Band	66
10. Wave Number Differences Between Features in the 7090 A Band	67
11. Parameters Resulting from Band Assignments	75
12. Character Table for the Point Group C_{2v}	81
13. Direct Products for the Point Group C_{2v}	81
14. Possibilities for Transitions.	83
15. Comparison of Cut-off and Thermodynamic Values	87
16. Wave-lengths, Frequencies, and Estimated Intensities of Features from 6559 A to 5362 A.	88
17. Wave-lengths and Frequencies of Outstanding Features from 5342 A to 4351 A	92

LIST OF ILLUSTRATIONS

Figure	Page
1. Gas System for Absorption Cell	29
2. Microphotometer Trace of the Band Near 6720 A at 420 Gauss	37
3. Microphotometer Trace of the Band Near 6720 A at 780 Gauss	38
4. Microphotometer Trace of the Band Near 6720 A at 1350 Gauss.	39
5. Microphotometer Trace of the Band Near 6720 A at 2000 Gauss.	40
6. Microphotometer Trace of Absorption Spectrum of Band Near 6720 A.	41
7. Microphotometer Trace and Assignments for the 7410 A Band.	53
8. Spacing versus g for a Perpendicular Transition and $V_2' = 8$	57
9. Spacing versus g for a Perpendicular Transition and $V_2' = 9$	58
10. Spacing versus g for a Parallel Transition and $V_2' = 8$	59
11. Spacing versus g for a Parallel Transition and $V_2' = 9$	60
12. Microphotometer Trace and Assignments for the 6720 A Band.	64
13. Microphotometer Trace and Assignments for the 7090 A Band.	68
14. Walsh's Correlation Diagram.	71
15. Microphotometer Trace of the Magnetic Rotation Spectrum of NO_2 from 6760 A to 5200 A . .	93

ABSTRACT

The magnetic rotation spectrum of a molecule is a spectrum obtained in the following way. Collimated, white light is passed successively through a polarizing prism, an absorption cell mounted along the axis of an electromagnet, and another polarizing prism. The gas to be studied is placed in the absorption cell. When the prisms are crossed no light passes, but when a magnetic field is produced along the direction in which the light travels, the plane of polarization may be rotated. Light then comes through the second prism and is focused upon the slit of a spectrograph. The resulting spectrum is the magnetic rotation spectrum. This technique has been very useful in the study of diatomic molecules. One advantage over the use of absorption spectra is that the magnetic rotation spectrum is a bright line spectrum. A second advantage is that a useful simplification of the spectrum is obtained, since only those lines which have pronounced Zeeman effects will appear. The use of magnetic rotation spectra in the study of polyatomic molecules has not received very much attention, although some studies have been made. It was thought that a method which is so useful in the case of diatomic molecules deserves reexamination in the case of polyatomic molecules. There is a great deal of current interest in the NO_2 molecule; the visible

system has not previously been analyzed, and this system has an intense magnetic rotation spectrum throughout the visible region. It was thus thought to be a natural choice for study. The objectives of the investigation may then be given as follows:

1. To determine the nature of the excited electronic state of NO_2 in the visible system.
2. To make vibrational assignments for the spectrum.
3. To say as much as possible about the resolvable rotational structure of the spectrum.
4. To make extensions of the theory of magnetic rotation to polyatomic molecules.
5. To explore the possibilities of magnetic rotation as a "general method" for polyatomic molecules.

Magnetic rotation spectra of NO_2 were observed under various conditions of magnetic field strength, NO_2 pressure, pressure of NO_2 plus argon, and at several temperatures. The magnet constructed for the investigation enabled field strengths up to 2000 gauss to be obtained. A Jarrell-Ash three-meter spectrograph was used which has a replica grating in a Wadsworth mounting. Ahrens prisms were used as the polarizing prisms. Absorption cells were made of pyrex tubing with pyrex windows, either waxed on with apiezon wax or fused directly onto the tubing. Windows for the cells had to be essentially free from strain and distortion. Samples of NO_2 were made by heating $\text{Pb}(\text{NO}_3)_2$.

The overall intensity of the magnetic rotation spectrum was found to increase with an increase in field strength. Up to the highest fields used the variation was found to be essentially proportional to the square of the field strength. This fact, coupled with the fact that no magnetic rotation spectrum exists in the ultraviolet system of NO_2 where the excited state is bent, and the results of recent magnetic resonance studies which show the electron spin to be decoupled in the ground state at a field of 3000 gauss, is shown to indicate a linear, $^2\Pi$ excited state for the visible system.

The great complexity of the visible system is shown to be easily understood in terms of a linear excited state. As a result of the Franck-Condon principle long progressions in the degenerate bending vibration of the excited state should appear. This explains the extent of the spectrum. The degenerate bending vibration results in vibrational angular momentum, $\ell \frac{h}{2\pi}$, quantized about the figure axis along with the electronic angular momentum. An energy given by $g\ell^2$ must be added to the rotational energy. Defining an effective $K = \Lambda + \ell$, it is shown that the complexity of the spectrum can be explained by using symmetric top selection rules. Since the number of possible ℓ values in a band is restricted by $\ell = \pm V_2', \pm(V_2'-2), \dots, \pm\begin{cases} 1 \\ 0 \end{cases}$, bands would be expected to decrease in complexity in the direction of higher wavelengths. This was found to be the case in the observed magnetic rotation spectrum. The abrupt breaking-off of band

structure observed in the spectrum, inexplicable in terms of convergence or of a decreasing Boltzmann factor in a non-linear molecule, is easily explained in terms of the above interpretation.

Assignments of V_2' , ℓ , and K'' , and the spin splitting were made for the bands at 7410 Å, 7090 Å, and 6720 Å. From these assignments values for g and $(A''-B'')$ were obtained. V_2' values for the 7410 Å, 7090 Å, and 6720 Å bands were assigned as 6, 7, and 8 respectively. Considering the ground state as an accidental symmetric top, the transition was found to be perpendicular; that is, the electric vector vibrates in a plane perpendicular to the unique axis of the top. The value of g obtained is about $6.9 \pm 0.1 \text{ cm}^{-1}$. The value of $(A''-B'')$ obtained is about $7.4 \pm 0.1 \text{ cm}^{-1}$, which is in good agreement with the value 7.62 cm^{-1} found from infrared work. The spin splitting was found to depend upon V_2' , decreasing from about 107 cm^{-1} for $V_2' = 6$ to about 98 cm^{-1} for $V_2' = 8$. This is interpreted as due to Λ losing some of its significance as the molecule vibrates with a greater amplitude, thus decreasing its interaction with the spin. Using the above assignments, band origins were estimated. From these band origins vibrational intervals were obtained. The 7090 Å band showed some indications of Fermi resonance so the 7410 Å and 6720 Å bands were used to estimate the vibrational interval. The result is about 710 cm^{-1} for the bending frequency. This value for ν_2' indicates the origin

of the system to be at about 9220 cm^{-1} or 10800 Å .

The results of the above analysis were compared with theoretical calculations of the ordering and symmetries of electronic states in triatomic molecules. It was concluded that the transition is due to elevation of an electron from a non-bonding orbital localized on the nitrogen atom to an anti-bonding π orbital. It is interesting that correlation diagrams showing how occupancy of orbitals by electrons affects the bond angle are consistent with a large increase in bond angle for this transition and thus consistent with a linear excited state. The same transition has been concluded by others to be responsible for the corresponding system in the nitrite ion.

A magnetic field effect was observed in which an increase in the number of features occurred with an increase in field strength. Also the intensities of some features were augmented with respect to others. No explanation of this effect is given.

Studies of the effect of an increase in pressure on the spectrum showed that the violet end of the magnetic rotation spectrum cut off abruptly. At low pressure the cut-off position was found to be at $3981 \pm 3\text{ Å}$. Magnetic rotation spectra are easily destroyed by diffuseness in the band structure. The abrupt cut-off of the magnetic rotation spectrum is attributed to the onset of diffuseness due to the predissociation limit corresponding to dissociation of NO_2

into NO and O. An increase in pressure either of NO₂ alone or of NO₂ plus an added foreign gas was found to move the violet cut-off position in the direction of longer wavelengths. This phenomenon is ascribed to a pressure-induced predissociation, that is a selective pressure broadening.

It is recommended that studies of the magnetic rotation spectrum of ClO₂ be made. The magnetic rotation spectrum of ClO₂ has never been observed. If one exists, its variation with field would be of great interest in view of arguments presented in this thesis. It is also suggested that magnetic rotation spectra be investigated as a means for detecting diffuseness in spectra, predissociation limits in particular.

CHAPTER I

INTRODUCTION

Although far from completed fields of investigation, the spectra of atoms and diatomic molecules are well understood. The problem of interpreting the spectra of polyatomic molecules, however, presents a very formidable task, the execution of which is being pursued with great vigor and interest both experimentally and theoretically. The electronic ground states of polyatomic molecules have been and are being studied by the methods of electron diffraction, infrared spectroscopy, and microwave spectroscopy, as well as by methods such as paramagnetic resonance and techniques depending upon nuclear properties. From these sources information is obtained about the rotational and vibrational levels, the electronic states, and the geometry of molecules in their electronic ground states. Calculations of thermodynamic properties can be made using this information; also this information aids in answering other questions of chemical significance.

In order to study excited electronic states of molecules, one uses electronic spectroscopy in one of its forms. In the case of polyatomic molecules the resulting spectra can be very complicated, and special techniques may often be required in their analysis, an example being the use

of polarized radiation and oriented crystals (1). An understanding of excited states in general and characterization of these states in particular cases are desirable both intrinsically and for the light they shed on the mechanisms of reactions involving excited electronic states (2).

Reactions of this nature are important in photochemistry, radiation chemistry, and the study of flames. The data may also be useful in calculating thermodynamic properties of substances at very high temperatures. The intrinsic value of an understanding of excited states lies in its test of the developing theories of molecular structure.

The study of the magnetic rotation spectrum of a molecule to investigate its electronic spectrum has yielded good results in the case of diatomic molecules. The magnetic rotation spectrum is a spectrum obtained in the following manner. White light, collimated by an optical system, is passed successively through a polarizing prism, an absorption cell placed in an electromagnet, and another polarizing prism. The gas to be studied is placed in the absorption cell, and the polarizing prisms are crossed so that no light passes. When a magnetic field is produced along the direction in which the light travels, the plane of polarization is rotated, and light comes through the second polarizing prism. This effect is known as the Faraday effect. The light coming through is focused on the slit of a spectrograph.

The spectrum is a bright line spectrum, and herein

lies one of its virtues when compared with absorption spectra. It is easier to detect what is on the film than to detect what is not on the film. The bright line character of the spectrum also allows the spectrum to be "integrated" over time on the film. It was this property of magnetic rotation spectra that enabled Loomis and his students (3,4,5,6,7) to make accurate determinations of the heats of dissociation of alkali molecules, since it was possible to follow progressions to higher vibrational states than can be observed in absorption spectra.

A second merit in the use of the magnetic rotation spectrum is the fact that it often leads to a simplification of the spectrum. This simplification is due to the restriction that only those lines which have a pronounced Zeeman effect will appear. Thus for diatomic molecules, for example, only transitions involving low J values will appear.

These properties of magnetic rotation spectra, the success of the method, and information obtained from studies of several interhalogen compounds by Cheng (8) using this method indicate that its possible use in studying polyatomic molecules should be explored. A previous attempt in this direction was made by Kusch and Loomis (9), but much has been learned about polyatomic molecules and magnetic rotation since their attempt. It is believed that a method as useful as this one has proved to be in the case of diatomic molecules deserves careful investigation in the case of polyatomic

molecules. The visible system of NO_2 has never been analyzed, and there is an intense magnetic rotation spectrum throughout the system. There is a great deal of current interest in this molecule, and it is thus a natural choice for study. The objectives of this research may then be given as follows:

1. To determine the nature of the excited electronic state of NO_2 in the visible system.
2. To make vibrational assignments for the spectrum.
3. To say as much as possible about the rotational structure of the spectrum that resolution will allow.
4. To make extensions of the theory of magnetic rotation to polyatomic molecules.
5. To explore the possibilities of magnetic rotation as a "general method" for polyatomic molecules.

CHAPTER II

REVIEW OF LITERATURE

Magnetic Rotation Spectra

The Faraday effect, the rotation of the plane of polarization of light in transparent, isotropic media by a magnetic field along the path of the light, was discovered by Michael Faraday (10) in 1845. This effect differs from the rotation of the plane of polarization by optically active substances in that when the light is reflected back along its path, the rotation is doubled rather than cancelled out. Following its discovery, extensive investigations of the effect were made by Becquerel (11), Verdet (12), and others. It was found that the angle of rotation, θ , depends upon field strength, H , and path length, l , through the medium in the following way:

$$\theta = V_{\lambda} H l, \quad (1)$$

where V_{λ} is a constant called the Verdet constant. Verdet attempted to construct a classical theory for the Faraday effect by relating V_{λ} to refractive index and the wave-length of the incident light.¹

¹A more extensive treatment of the history of the Faraday effect and the development of its classical theories is given by Cheng (8).

Macaluso and Corbino (13) found that sodium vapor exhibited very large rotations in the immediate vicinity of the D lines. Rhigi (14,15) showed that in gaseous I_2 , Br_2 , and NO_2 there is an unusually large Faraday effect in regions where the absorption spectra are most intense. The study of magnetic rotation spectra as distinct from the ordinary Faraday effect dates from these investigations.

The discovery of the Zeeman effect and its theoretical interpretation enabled Larmor (16), Voigt (17), Zeeman (18), and others to give as accurate a theoretical approach to the theory of magnetic rotation near absorption lines as was possible using classical theory.

It was R. W. Wood (19) who initiated actual measurements on magnetic rotation spectra in his studies on Na_2 in sodium vapor which began in 1895 and continued until 1909. In 1928 Loomis (3) made the observation that the magnetic rotation lines in the blue-green system of Na_2 correspond to band heads in the absorption spectrum. He was able to follow the spectrum to vibrational levels close to the convergence limit. Loomis and his associates (4,5,6,7) then used this method in order to obtain precise values for the dissociation energies of other alkali metal molecules from their $^1\Pi \leftarrow ^1\Sigma$ systems. In the $^1\Sigma \leftarrow ^1\Sigma$ system of Na_2 no magnetic rotation spectrum was expected because of the absence of a Zeeman effect for $^1\Sigma \leftarrow ^1\Sigma$ transitions, but a magnetic rotation spectrum does exist. This difficulty was resolved by

Fredrickson and Stannard (20), who showed that a perturbation of a few of the upper levels of the upper state was responsible for the spectrum.

In 1931 Wood and Dieke (21) studied the magnetic rotation spectrum of NO_2 and reported the following:

It was found that with NO_2 a remarkable simplification occurred. But in this case also the simplified magnetic rotation spectrum is very complicated and we have not yet succeeded in analyzing it, further experimental work under higher dispersion being required before an analysis can be attempted.

With NO_2 in a bulb of 3 cm in diameter at rather low pressures² (only slight trace of yellow by transmitted light), a rotation spectrum appeared with a field strength about equal to that of an ordinary permanent magnet. As the field increased, some of these lines disappeared and new lines were developed. The disappearance seems to be a real phenomena and not due to a 90° rotation, as observations with the double quartz wedge of R- and L-quartz indicated that rotations involved were only of a few degrees.

Wood and Dieke found that Na_2 behaved in a similar manner with a variation in field. They attributed this variation to the importance of low J values in contributing to the magnetic rotation at low fields and to an increased contribution of higher J values as the field becomes stronger.

In 1939 Kusch and Loomis (9) investigated the magnetic rotation spectra of SO_2 and CS_2 in order to see if a useful simplification of the very complicated structure of the absorption spectra of polyatomic molecules would result. CS_2 has an absorption spectrum in the region between 3900 Å and 2750 Å. Kusch and Loomis found an intense magnetic rotation spectrum in the region 3355 - 3640 Å, and a very

much weaker one in the region 3125 - 3250 Å. They note that the magnetic rotation spectrum occurs in that region where the absorption bands are sharp and that no magnetic rotation occurs in the short wave-length region where the bands are diffuse and irregular. Good correlation was found between magnetic rotation lines and band heads in the absorption spectrum, and the authors attribute the spectrum to a ${}^1\Pi \leftarrow {}^1\Sigma$ type transition. This assignment attributes both the ground and excited states to linear configurations with orbital angular momentum about the figure axis in the excited state, giving rise to a magnetic moment coupled to the figure axis. SO_2 has an intense absorption spectrum in the region between 2600 Å and 3900 Å which is about ten times as intense as the corresponding absorption system in CS_2 . Kusch and Loomis found a magnetic rotation spectrum in the region 2939 - 3164 Å which is much less intense than that of CS_2 . This spectrum is apparently due to some kind of perturbation, and the authors found their results confusing. HCHO was also investigated. HCHO has an absorption spectrum in the region 2750 - 3750 Å. A magnetic rotation spectrum was found for the band at 3260 Å only. No regularities were apparent. The authors also assert that although acetaldehyde and acrolein have well defined absorption spectra in the near ultraviolet, neither of these two molecules exhibits a magnetic rotation spectrum. They mention that ozone, which shows strong absorption between 2900 Å and 3660 Å, does not have a magnetic

rotation spectrum.² In discussing Wood and Dieke's work on NO_2 , the authors assert, "This spectrum was readily obtained but consisted of an apparently hopeless confusion of structure which gave no useful simplification of the absorption spectrum." The paper is ended in a pessimistic note as far as the application of magnetic rotation to polyatomic molecules is concerned.

The modern quantum mechanical theory of magnetic rotation spectra was first developed for atoms in 1929 by Rosenfeld (22). For molecules the quantum mechanical theory was first attempted by Kronig (23) and later extended by Serber (24) and by Carroll (25). A discussion of the theory will be presented later. It should be mentioned for completeness that Carroll, too, expressed pessimism with respect to the value of magnetic rotation spectra in studying polyatomic molecules. He concluded that in the polyatomic case, perturbations and other complexities of spectrum would appear rather than the simple features.

Nitrogen Dioxide

Ground State.--Nitrogen dioxide, NO_2 , is a dark red gas which exists in equilibrium with its dimer, N_2O_4 . By means of magnetic susceptibility measurements, Havens (26) has demonstrated that NO_2 contains one unpaired electron. There has been a great deal of controversy as to the geometry and

²In private communication, Dr. W. H. Eberhardt attributed this fact to the diffuseness of the band structure.

the vibrational and rotational constants of the electronic ground state, but the results of the most recent electron diffraction work and studies of the infrared spectrum are now in good agreement. The electron diffraction studies of Claesson, Donahue, and Shomaker (27) give an internuclear distance of 1.20 ± 0.02 A and an angle of $132 \pm 3^\circ$. The infrared studies of Moore (28) give for these same parameters the values 1.188 ± 0.004 A and $134^\circ 4' \pm 15'$ respectively. Moore's paper also contains a good account of the vibrational and rotational constants. In his rotational analysis, Moore found that to a good approximation, NO_2 behaves as a symmetric rotor, and he represents the rotational levels by the formula,

$$F(J,K) = BJ(J+1) + (A-B)K^2 - D_J J^2(J+1)^2 - D_K K^4. \quad (2)$$

His rotational constants as well as vibrational constants defined by the equation,

$$G(v_1, v_2, v_3) = \sum_{i=1}^3 \omega_i (v_i + \frac{1}{2}) + \sum_{i=1}^3 \sum_{j=1}^3 x_{ij} (v_i + \frac{1}{2})(v_j + \frac{1}{2}), \quad (3)$$

are given in Tables 1 and 2. It is encouraging that four absorption lines predicted by Moore's analysis have been found in the microwave spectrum by Bird (29).

The microwave spectrum of NO_2 was first observed by McAfee (30,31). It is apparently not easy to interpret, particularly with respect to hyperfine structure. Its only interest to this investigation is that it indicates the ground

Table 1. Vibrational Constants for NO₂

Constant	Value cm ⁻¹
ω_1	1361.4 ± 1.7
ω_2	770.2 ± 6.6
ω_3	1668.6 ± 1.7
ν_1	1322.5 ± 1.7
ν_2	750.9 ± 0.4
ν_3	1616.0 ± 0.2
x_{11}	-7.1 ± 0.3
x_{12}	-16.0 ± 3.3
x_{13}	-33.4 ± 0.1
x_{22}	-8.1 ± 3.3
x_{23}	-8.2 ± 3.3
x_{33}	-15.9 ± 0.2

Table 2. Rotational Constants for NO₂

Level	B cm ⁻¹	A - B cm ⁻¹	D _j (X10 ⁵) cm ⁻¹	D _k (X10 ³) cm ⁻¹
Ground	0.429 ± 0.002	7.62 ± 0.05	1.0 ± 0.2	5.8 ± 1.2
ν_2	---	7.92 ± 0.05	---	5.4 ± 1.2
$2\nu_1 + \nu_3$	0.422 ± 0.002	---	1.0 ± 0.2	---
$3\nu_3$	0.422 ± 0.002	---	1.0 ± 0.2	---
$3\nu_1 + \nu_3$	0.419 ± 0.003	---	---	---

state to be a 2A_1 state with the odd electron localized on the nitrogen (32).

Castle and Beringer (33) made a study of paramagnetic resonance in NO_2 . They found that the electron spin is essentially free in a magnetic field of about 3000 gauss. In other words, they interpret the spectrum in terms of a Paschen-Back effect.

Ultraviolet Systems.--Two regions in the ultraviolet exhibit absorption systems. Price and Simpson (34) report a Rydberg series occurring between 1600 Å and 1350 Å. The other absorption system lies between 2600 Å and 2000 Å and has been studied extensively by Herrmann (35); Ionescu (36); Harris, Pearse, Benedict, and King (37); and Harris and King (38). Harris, Pearse, Benedict, and King attempted a vibrational analysis and obtained 523 cm^{-1} and 714 cm^{-1} for the vibrational intervals in the upper state. For intervals in the lower state, they obtained the values 749 cm^{-1} and 1319 cm^{-1} which are in good agreement with values obtained later by Moore (28) in his infrared work. Harris and King (38) attempted a rotational analysis of the band at 2491 Å and obtained an angle of 154° for both the lower and upper states and an internuclear distance of 1.28 Å and 1.41 Å respectively.

It was found by Henri (39) that a predissociation phenomenon exists in this ultraviolet system, the bands becoming diffuse and broad at 2459 Å and remaining so up to 2200 Å. Henri asserts the predissociation to be due to

dissociation into NO in its ground state and an activated oxygen atom, probably in the metastable 1D state. Of great interest to this investigation is the attempt of Herrmann (35) to use magnetic rotation to study this system. He was unable to find any trace of magnetic rotation.

Visible System.--The absorption spectrum in the visible region starts at about 3500 A and has been followed up to 9000 A. No detailed analysis of this system has previously been given. Curry and Herzberg (40) suggest as a possible explanation for the great complexity of this system that chiefly higher vibrational levels in the upper state are excited as a result of the Franck-Condon principle. Working upon this assumption they followed the spectrum to longer and longer wave-lengths. They found, "a rather simple series of bands starting at about 8900 A and extending to shorter wave lengths." The distance between main bands was found to be $740 - 730 \text{ cm}^{-1}$, which they asserted must be a vibrational frequency of the upper state. Dixon (41) has studied the absorption of NO_2 in the visible region spectrophotometrically. He concluded that the maxima are separated by $700 \pm 100 \text{ cm}^{-1}$ and attributes this to the excited state. Hall and Blacet (42) have used an ingenious method for separating the absorption spectra of NO_2 and N_2O_4 in the range 2400 - 5000 A. Their results show that N_2O_4 does not contribute to the absorption spectrum above 4000 A.

Predissociation was also found in the visible system

by Henri (39). The predissociation limit assigned by Henri is at 3700 A, but Frank, Sponer, and Teller (43) assert that at higher dispersion, the beginning of unsharpness is at 4000 A. This limit corresponds to dissociation of the NO_2 into a normal NO molecule and a normal oxygen atom, both in their ground states. Kondratiew and Polak (44) found evidence of a pressure-induced predissociation, that is, a selective broadening of bands with an increase in pressure. They found that Beer's law does not hold for regions of predissociation, and deviations increase with increasing pressure of the gas, original or foreign.

Norrish (45) studied the fluorescence of NO_2 . He found that NO_2 undergoes photochemical dissociation into NO and O_2 by light of 3650 A, but that light of 4300 A has no effect. This fact tends to support Henri's assertions with respect to the predissociation limit. More recent work on the fluorescence of NO_2 has been done by Neuberger and Duncan (46). Interesting results were obtained with respect to life-times, but nothing conclusive resulted.

CHAPTER III

THEORETICAL CONSIDERATIONS

Plane polarized light travelling through an isotropic medium may be considered as a superposition of two components which are circularly polarized in opposite directions. If these components are propagated at different velocities, that is, if they have different refractive indices in a given medium, the plane of polarization is rotated when the light travels through the medium.¹ This may be expressed mathematically in the following way:

$$\theta = \pi v \ell (n_- - n_+), \quad (4)$$

where θ is the angle through which the plane of polarization is rotated; ℓ is the path length through the medium; v is the frequency in wave numbers of the incident radiation; and n_- and n_+ are respectively the refractive indices of the left and the right-handed components of circularly polarized light. The theory of the Faraday effect is thus a description of how

¹If one of the components is absorbed more than the other, elliptically polarized light will result rather than plane polarized light. In this case complete extinction of the light can not be accomplished by means of a polarizing prism. When the prism is rotated, the intensity, however, will go through a minimum and a maximum. The angle of rotation is then said to be determined by the difference in angle between the plane of polarization of the entering light and the plane containing the major axis of the ellipse.

the magnetic field interacts with the medium so as to make n_- and n_+ different. Refractive index is related to other molecular properties through the Kramers dispersion formula, which may be written as follows:

$$n = 1 + \frac{e^2 N}{2\pi m Q} \sum_{j,k} \frac{f_{jk}}{v_{jk}^2 - v^2} \exp\left(-\frac{W_j}{kT}\right), \quad (5)$$

where N is the number of molecules per cubic centimeter; W_j is the energy of an initial state for the electronic transition; v_{jk} is the frequency of the transition from the state j to the state k ; and f_{jk} is the oscillator strength of the transition from j to k . f_{jk} is related to the matrix elements of the dipole moment between the two states. A magnetic field may, therefore, affect the refractive index of a medium in three ways. These ways are:

1. By changing v_{jk} through the Zeeman effect.
2. By changing f_{jk} through a perturbation of the matrix elements of the dipole moment.
3. By changing the population in the various ground states of the transitions, that is, through its effect on $N_j = \frac{N}{Q} \exp\left(-\frac{W_j}{kT}\right)$.

Serber (24) uses a perturbation method in approaching this problem. Assuming the magnetic field and the path of the light to be along the Z axis, Serber writes the expression for the rotation of the plane of polarization per centimeter, φ^* ,

*Serber labels this quantity Θ . It is labeled φ here in order to avoid confusion with Θ as used previously in the text.

in the following way:

$$\varphi = CB \sum_{n,n'} \tau(n'n) [P_x(nn') P_y(n'n)] \exp\left(-\frac{W_n}{kT}\right), \quad (6)$$

where $B = \frac{N}{\sum_n \exp\left(-\frac{W_n}{kT}\right)}$ and $C = \frac{4\pi^2 v^2 i}{ch}$.

$$[P_x(nn') P_y(n'n)] = P_x(nn') P_y(n'n) - P_y(nn') P_x(n'n),$$

where $P_x(nn')$ and $P_y(nn')$ are the elements of the x and y components of the electric dipole moment in the presence of the field.

$$\tau(n'n) = \frac{1}{[v^2 - v^2(n'n)]^2},$$

where $v(n'n)$ has the same significance as v_{jk} mentioned above. Serber then expands the quantities P_x , P_y , $v(n'n)$, W_n , and B in power series of the following form (using P_x as an example):

$$P_x = P_x^0 + H P_x^{(1)} + \dots$$

Assuming $v - v(n'n)$ large compared to the Zeeman splitting and considering terms linear in the magnetic field intensity, H , Serber obtains the following expression:

$$\begin{aligned} V = \frac{\varphi}{H} = & CB^0 \sum_{n,n'} \left\{ \tau^0(n'n) ([P_x^0(nn') P_y^{(1)}(n'n)] \right. \\ & + [P_x^{(1)}(nn') P_y^0(n'n)]) \\ & + 2v^0(n'n) v^{(1)}(n'n) \tau^0(n'n)^2 [P_x^0(nn') P_y^0(n'n)] \\ & \left. - \left(\frac{W_n}{kT}\right) \tau^0(n'n) [P_x^0(nn') P_y^0(n'n)] \right\} \exp\left(-\frac{W_n^0}{kT}\right). \end{aligned} \quad (7)$$

There are two types of experiment that the theory must consider. One is rotation studied in transparent regions of the spectrum, using high pressures and monochromatic radiation. The other uses low gas pressures, continuous radiation, and is concerned with rotations in the immediate vicinity of absorption lines. It is this latter case that applies to magnetic rotation spectra. Therefore, for the case of magnetic rotation spectra the above equation for V reduces to:

$$V = \frac{2CB \sum_{m,m'} v(n'n) v^{(1)}(n'm'; nm) [P_X(nm; n'm') P_Y(n'm'; nm)] \exp\left(-\frac{W_n}{kT}\right)}{[v^2 - v(n'n)^2]^2}, \quad (8)$$

since this term becomes very much larger than the others as v approaches $v(n'n)$. Thus the rotation depends only upon the Zeeman effect, the other factors being negligible. By examining the dispersion curves for a normal Lorentz doublet, a good qualitative description of magnetic rotation near absorption lines can be obtained (25). Rotation takes place symmetrically (in this case) about the no-field position, essentially on the "shoulders" of the line. If the line is very diffuse, such as in the case of excessive pressure broadening, the intensity of light coming through the system will approach zero, since rotated light will be unable to get out from under the line and will be absorbed.

Since the magnetic rotation spectrum of a molecule depends upon its Zeeman effect, the case in which the Zeeman

effect goes over into a Paschen-Back effect should be considered. If the molecule has orbital angular momentum and electron spin, these two angular momenta will be coupled to each other by their magnetic interaction. Depending upon the magnitude of the interactions and the manner in which all the angular momenta are combined, molecules fall into a number of classifications called Hund's coupling cases. A discussion of these cases for diatomic molecules is given by Herzberg (47). Magnetic moments due to electronic angular momenta are about two thousand times as great as magnetic moments due to rotation of the nuclear framework or nuclear spin. Thus, except where hyperfine structure can be studied, magnetic moments in molecules may be attributed to electronic angular momenta alone. For case (a) coupling in diatomic molecules and "weak" fields, the following expression is found for the Zeeman splitting:

$$\bar{\mu}_H^H = \frac{(\Lambda + 2\Sigma)(\Lambda + \Sigma)M}{J(J + 1)}\mu_{0H}, \quad (9)$$

where Λ is the component of orbital angular momentum about the figure axis; Σ is the component of electron spin about this axis; $J(J + 1)$ is the square of the total angular momentum; and M is the component of total angular momentum along the field direction.² In case (b) coupling, the coupling between the spin and the orbital motion is much

²These angular momenta are in units of $\frac{h}{2\pi}$.

weaker, and the Zeeman splitting is given by:

$$\bar{\mu}_H^H = \frac{\Lambda^2}{\sqrt{K(K+1)}} \cos(K,J) + 2\sqrt{S(S+1)} \cos(S,J) \frac{M\mu_0^H}{\sqrt{J(J+1)}}, \quad (10)$$

where $K(K+1)$ is the square of the total angular momentum apart from spin. If the magnetic field is sufficiently strong, the spin can be decoupled from the orbital angular momentum (or other angular momentum), and both will be quantized separately along the field direction. This is called the Paschen-Back effect. Molecules having case (b) coupling are more easily decoupled by the field than those having case (a) coupling, and when the multiplet splitting is small compared to the Zeeman splitting, the latter is given by:

$$\bar{\mu}_H^H = \frac{\Lambda^2 M_K}{K(K+1)} \mu_0 + 2M_S \mu_0. \quad (11)$$

The selection rules that hold in this case are the following:

$$\Delta M_K = 0, \pm 1; \Delta M_S = 0.$$

The electron spin in a $^2\Sigma$ state is coupled only to rotation of the nuclear framework and nuclear spin; this coupling is very weak. Thus for a $^2\Sigma$ state no Zeeman splitting is expected, and no Zeeman effect has been observed. Therefore, there is no magnetic rotation spectrum for $^2\Sigma$ states except in cases of perturbations (20). Non-linear polyatomic molecules approximate case (b) coupling because there is no

axis upon which orbital angular momentum can be quantized. They behave in a manner similar to $^2\Sigma$ states (48). This fact will be of great value in interpreting the magnetic rotation spectrum of NO_2 .

CHAPTER IV

APPARATUS AND CALIBRATION

The source of white light for the optical system was a 100-watt concentrated arc, manufactured by the Sylvania company. This arc emits white light by ion bombardment of zirconium oxide in an atmosphere of argon and is powered by a D. C. power supply, which is essentially a rectifier supplying a high voltage for starting the arc and a lower voltage (of about 15 volts) for maintaining the arc. The light source obtained in this way has a diameter of 1.5 mm, which is sufficiently close to a point source for the needs of the experiment. The spectrum of the source is a continuum in the visible region with an intensity of about 400 watts per square cm at 6000 Å. The intensity drops off in the direction of shorter wave-lengths until at 4000 Å it is about 0.3 watts per square cm. In the direction of higher wave-lengths the intensity increases, but emission lines from the source, mostly argon lines with some zirconium lines, appear. Between 6000 Å and 7000 Å there are a few of these lines, and between 7000 Å and 10000 Å there are many lines.

In order to obtain parallel light, a convex achromatic lens was placed in the system at a position such that the light source was at the focal point. An aperture was placed next to the lens so that light would go through the center

of the first Ahrens prism, which was the next element in the optical system. Polarized light from the Ahrens prism then passed through the cell containing the sample. On the other side of the sample cell, another aperture was placed in order to select the light coming straight through the cell and so that the light would go only to the center of a second Ahrens prism. In magnetic rotation experiments the second Ahrens prism was set to extinguish the light coming from the first prism when the magnetic field was off. With the application of the field, rotated light came through and was allowed to fall on another achromatic lens which focused it upon the slit of the spectrograph. A cylindrical lens was placed between the achromatic lens and the slit. The purpose of this cylindrical lens was to concentrate the light along the length of the slit.

Absorption cells were made of pyrex tubing with pyrex windows. Earlier cells were made by sealing the windows on the tubing with apiezon W wax, but later they were fused on. The difficulty with fusing windows on the cell earlier was the fact that strain and distortion rotate the plane of polarization of the light and interfered with the experiment. This difficulty was later overcome. An attempt was made to minimize reflection from the walls of the tube for the same reason. Cells were of two types: long cells (56 cm) filled by means of a gas system through a side arm in one end of the tube, and short cells (20 or 16 cm in length), which contained

samples sealed inside. The diameter of the tubing varied depending upon the nature of the experiment, but generally the widest possible tubing that would fit inside the magnet was used. For most experiments the long cells were used.

The electromagnet was designed to give a maximum field of about 2000 gauss and to have good heat transfer properties. It consists of six copper spools, each wrapped with thirty pounds of B and S 14 gauge magnet wire. Each spool was made of two copper discs $\frac{3}{32}$ inches in thickness and 10 inches in diameter. Holes were cut in these discs so that they could just slip over a copper pipe with an outside diameter of 2.375 inches. The discs were soldered on the copper pipe at a distance of $2\frac{13}{16}$ inches apart with $\frac{1}{8}$ inch of pipe extending beyond each disc. Magnet wire was wrapped on these spools manually. These sections were slipped over a condenser-type arrangement of metal tubes, consisting of a brass tube $25\frac{1}{2}$ inches long inside a copper tube $22\frac{1}{2}$ inches long. The tubes were soldered together so that there was space for water to circulate between them. An inlet and an outlet for water were attached. The magnet was cooled by circulating water through the central part by means of the condenser arrangement and by blowing air over the outside of the sections. The magnet was made in sections to allow better circulation of air and to give a larger surface from which heat could escape. Considerations of the heat transfer properties of the magnet were of great importance because of the long exposure times

during which the field had to be maintained. During the course of the investigation the circuit for the magnet was changed several times. In every modification of the circuit, resistors in parallel were used to control the current going through the sections. These resistors were connected into the circuit by means of switches on a control panel. In the most recent modification of the circuit, all of the sections were wired in parallel through shorted plugs which allowed the number of sections used to be varied. Calibration of field strengths was made by measuring the rotation of the plane of polarization in water and using the known Verdet constant for water. Fields as high as 2000 gauss and as low as 140 gauss could be obtained.

The spectrograph used was a three-meter replica grating instrument, manufactured by the Jarrell Ash Company (J. A. 78). It is a stigmatic instrument, using a Wadsworth mounting. The four-inch replica grating has 15,000 lines per inch, giving a linear dispersion of 10.9 Å/mm in the first order. A mask was used on the grating. For spectra in the region of wave-lengths below 6800 Å, Kodak 103-F film was used, and for regions of wave-lengths greater than 6800 Å, Kodak HIR-408 film was used. In both cases the films were developed for three minutes in Kodak D-19 developer. 103-F films were left in the stop solutions for several minutes in order to allow the backing of the film to be removed more easily. Films were left in the fixer for from five to ten minutes, washed

for about one-half hour, and hung to dry. Exposure times depended upon the slit width, the field strength used, the region of the spectrum, and the relative intensity of the features of interest. They ranged from one-half hour to forty hours. Exposure times using HIR film were about four times as long as those using 103-F film under corresponding conditions. More will be said about exposure times with respect to specific experiments.

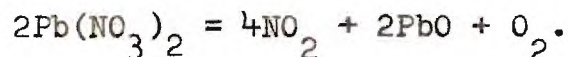
Calibration for the measurement of wave-lengths was accomplished by introducing an iron arc into the optical system by means of a mirror which could be inserted and removed without disturbing the rest of the system. The iron electrodes for the arc were mounted on a CENCO arc support. Since the spectrograph allows a number of spectra to be taken on the same film (the number depending upon the slit height used), the iron arc spectrum was easily placed on the film. In order to correct for possible lateral displacements when the "plate position" was changed, a helium Geissler tube was introduced into the system by means of a mirror similar to that used for the iron arc. A helium spectrum was superimposed on both the spectrum to be studied and the iron arc, using a slit height slightly longer than for the other spectra. The few helium lines that appeared could be easily located because of their greater length and served to correct for lateral displacements on the film and on the photometer traces. In the region above 6800 A, the use of the helium

Geissler tube was not necessary, because emission lines from the light source appeared on the film in spite of the crossed polarizing prisms. These lines were used in the same way as the helium lines.

Microphotometer traces of the films were made, using a recording microphotometer built here at Georgia Tech. The film carrier and optical assembly have been described by Wilson (49), and the other features have been described by Trawick (1). An intermediate scanning speed was used, such that a dispersion of approximately 20.5 Å per inch was obtained for the traces. By superimposing the iron arc and the spectrum on the traces, the wave-lengths of features could be determined by measuring their distance from nearby iron lines. Additive corrections were determined using the helium or argon lines. An architect's scale with 48 divisions per inch was used in measuring distances. It was possible to measure iron lines from other iron lines nearby to a few tenths of an Angstrom unit. The error increases with distance. The absolute measurement of the wave-lengths of features was probably not quite as precise because of the use of wider slits and the errors in corrections. Differences between features were probably more precise. Wave-lengths were converted into frequencies in wave numbers using Kayser's tables (50).

NO_2 was prepared by heating $\text{Pb}(\text{NO}_3)_2$ mixed with sand and condensing the gas as N_2O_4 in a dry ice-methanol bath.

The equation for the reaction is as follows:



The sand was used to react with the PbO to prevent it from attacking the glass of the containing tube. As the $\text{Pb}(\text{NO}_3)_2$ heated up, the system was pumped out to remove any moisture present. When a sufficient quantity of N_2O_4 was obtained, a vacuum pump was allowed to pump on the sample in the gas system for the sample cell. The N_2O_4 obtained in this manner was a white crystalline material. Occasionally a blue solid would form (N_2O_3). In this event the sample was discarded. A diagram of the gas system for the long sample cells is given in Figure 1. In the gas system apiezon stopcock grease was used. The system could be pumped out to an extent measured by a thermocouple vacuum gauge (30 microns).

The pressure of NO_2 in the sample cell was determined by fixing the temperature of a methanol bath in a Dewar flask and immersing the sample of N_2O_4 . Using vapor pressure data, the NO_2 pressure could be found. High pressures and total pressures including foreign gases such as argon, which was added in some experiments, were measured using a glass spiral pressure gauge. This pressure gauge was made by constructing a spiral of thin-walled glass. A mirror consisting of a silvered cover glass was glued to the end so that it would rotate when the pressure changed. Since it was found that this device worked best as a null reading instrument, it was

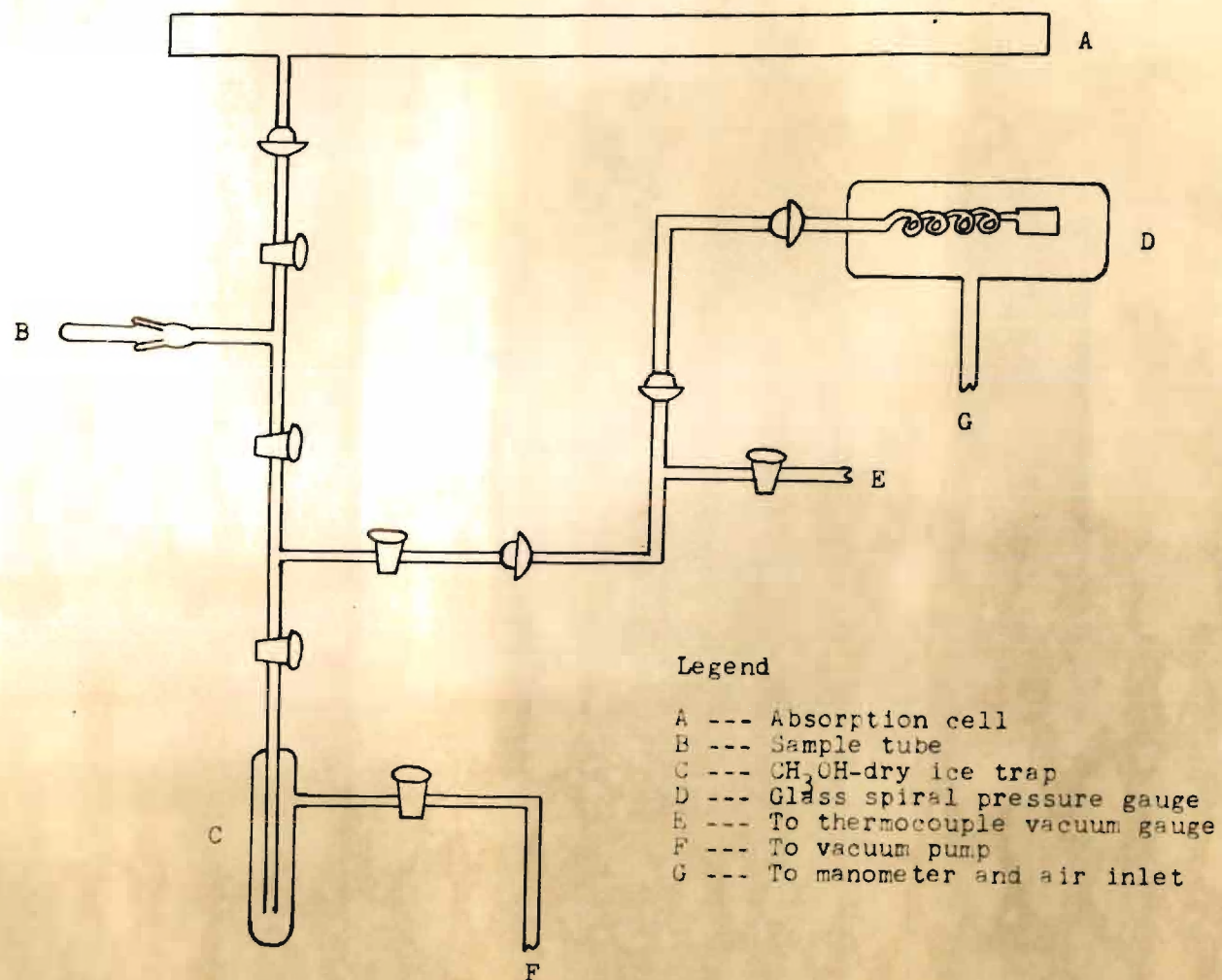


Figure 1. Gas System for Absorption Cell

placed inside a glass envelope attached to a vacuum pump, a mercury manometer, and a valve for allowing air to enter. Using a lens with a focal length of one meter and a light, a spot of light with a dark cross could be reflected from the mirror onto a fixed scale. The pressure inside the glass envelope and the pressure inside the spiral, which was connected to the gas system, had to be the same for the light spot to be in the null position. The pressure inside the system could be measured by adjusting the pressure in the glass envelope to the same value and reading the manometer. Similarly the gas system could be filled to a desired pressure. The limit of sensitivity of this manometer was approximately 1 - 2 mm Hg.

In a few experiments spectra were taken at different temperatures. This was accomplished by using a condenser-type sample cell with cooled water circulating through it or allowing the inside of the magnet to heat up by cutting off the regular cooling water. The temperature was determined by measuring the temperature of water leaving the condenser-type cell in the case of cooling the cell and by measuring the temperature of water inside the condenser arrangement of the magnet in the case of heating the cell. In studies of absorption, electrical heating was used, and measurements of temperatures were made with a thermocouple and potentiometer.

CHAPTER V

DESCRIPTION OF EXPERIMENTS

Magnetic rotation spectra of NO_2 were studied under a variety of conditions. The conditions that could be varied in the course of the investigation were NO_2 pressure, total pressure of NO_2 plus a foreign gas, magnetic field intensity, sample temperature, slit width, and exposure time.

Spectra were taken at a series of NO_2 pressures using a wide slit (0.5 mm) and one hour exposure times in order to find the optimum pressure for the middle visible region. It was soon apparent that the cut-off point on the violet end of the spectrum was quite sensitive to NO_2 pressure. As the pressure increased, the intensity of the spectrum increased in the red regions, but the violet cut-off of the spectrum appeared at longer and longer wave-lengths. Experiments were then made at a constant NO_2 partial pressure of about five millimeters and a number of total pressures of NO_2 and argon. With an increase in total pressure, the violet cut-off moved toward longer wave-lengths without appreciably changing the intensity of the bands in the red region. Total pressures above 100 mm were found to decrease the intensity of the entire magnetic rotation spectrum because of pressure broadening. At a total pressure of 210 mm only a few of the most intense features appeared, and pressures higher than this

were found to destroy the spectrum. A search was made to find the limiting cut-off wave-length on the violet end at low pressure. The spectrum was overexposed to insure that the end of the spectrum would be observed. The point at which the intensity of the light source dropped off considerably was clearly visible on the film because of the blackening due to background radiation. Moving in the violet direction, the end of the magnetic rotation spectrum was reached before this point. The violet cut-off point for the spectrum was found to be at $3981 \pm 3 \text{ \AA}$.

Prominent features were measured, using spectra made with a slit width of 0.5 mm, from 6600 \AA to 4350 \AA , and their wave-lengths, frequencies, and a rough estimate of their intensities were tabulated. Spectra with finer slits were also taken in this region. Very long exposures were needed for fine slits; for example, forty hours of exposure time were required with a 60 micron slit width. Also the reciprocity law began to fail under these conditions. An experiment was made to find the differences between a spectrum taken at 5°C and one taken at 34°C .

Studies with slit widths of 100 microns were made in the region of wave-lengths longer than 6600 \AA . It has been reported (40) that by increasing the pressure of NO_2 , the absorption spectrum can be followed up to 9000 \AA . Therefore an attempt was made to go as far as possible into the infrared. Bands were found and developed nicely up to 7475 \AA .

Some indications of a band were found near 7900 Å, but the features were not well developed, and there existed some ambiguity in that some of the features (if not all) may be due to emission lines from the source. A point of diminishing returns was reached, because further increases in pressure began to decrease the intensity through pressure broadening. Exposure times in this region were already very long because of the low sensitivity of the film.

The variation of the magnetic rotation spectrum with changes in magnetic field intensity was investigated. So that the spectra at different fields would be of comparable intensity, they were studied at equal values of tH^2 , that is, of exposure time multiplied by the square of the field strength. The argument for using equal values of tH^2 is that the intensity of light is proportional to the square of the electric vector. If the plane of polarization is taken to be the plane in which the electric vector vibrates, the intensity of light coming through a polarizing prism depends upon the square of the component of the electric vector allowed to pass. When the prisms in the experiment are crossed, the component of the electric vector allowed to pass is zero; but after the plane of polarization is rotated through an angle, θ , a non-zero component comes through the polarizer. It may easily be shown that this component is proportional to $\sin \theta$. Therefore the intensity is proportional to $\sin^2 \theta$ which for small rotations may be replaced by θ^2 . Since θ is proportional

to H , intensity is proportional to H^2 and the exposure to tH^2 . An experiment was made in which two spectra of the same sample were obtained, one at a field strength of 1300 gauss and an exposure time of 50 minutes and the other at a field of 780 gauss and an exposure time of two hours and twenty minutes. The slit width in both cases was 0.5 mm. A visual examination of the overall intensities on the film justified the use of equal values of tH^2 . Using a 100 micron slit, spectra were taken at 420, 780, 1350, and 2000 gauss. Small cells that fitted entirely into two sections of the magnet were also used at a number of different field strengths in order to eliminate end effects at points where the field falls off.

In addition to magnetic rotation spectra, a number of absorption spectra of NO_2 were taken. The effect of varying the sample temperature was also studied in absorption.

CHAPTER VI

RESULTS AND DISCUSSION

The absorption spectrum of NO_2 is extremely complicated. The magnetic rotation spectrum is also complicated, but it does appear to offer some simplification when compared to the absorption spectrum. It is very bright and extends over a large region of the spectrum. Features are grouped into complexes or "bands" which seem to increase in complexity in the direction of shorter wave-lengths. The abrupt cut-off of the spectrum on the violet end has already been described in Chapter V. Its limiting position at low pressure was found to be at a wave-length of $3981 \pm 3 \text{ \AA}$. 4000 \AA has been assigned as the predissociation limit corresponding to dissociation of NO_2 into NO and O , both in their ground states (43). Since predissociation manifests itself by a diffuseness in the band structure, the abrupt cut-off of the magnetic rotation spectrum is easily understood in terms of the ease with which diffuseness destroys the spectrum. Similarly, the progressive shift in the cut-off position towards longer wave-lengths with an increase in pressure can be interpreted in terms of a pressure-induced predissociation, that is, a selective pressure broadening. An effect of this nature has been noticed in this region by Kondratiew and Polak (44).

The variation of the magnetic rotation spectrum with

a change in magnetic field strength must be discussed from two aspects. These are the variation of the overall intensity of the spectrum and the variation of relative intensities of features, including their appearance or disappearance. With respect to the overall intensity of the spectrum, it has already been pointed out that the intensity is essentially proportional to the square of the field strength. This seems to be the case even at the highest field strength used, about 2000 gauss. With respect to the second aspect of the variation, it has been found that an increase in the number of features developed occurs with an increase in field, or at least their intensities relative to already developed features are greatly augmented. Relative intensities of other features may also vary somewhat. In Figures 2, 3, 4, and 5, microphotometer traces of the band near 6720 Å at fields of 420, 780, 1350, and 2000 gauss respectively are shown, which illustrate these points. In Figure 6 a photometer trace of the absorption spectrum of the same band is shown for comparison. It will be noticed that at higher fields the band resembles the absorption spectrum more closely than at low fields. Nevertheless, even at higher fields the magnetic rotation spectrum and the absorption spectrum are not superimposable.

It has been shown in the section on theoretical considerations that if there is no quantized electronic angular momentum in a molecule other than electron spin, the

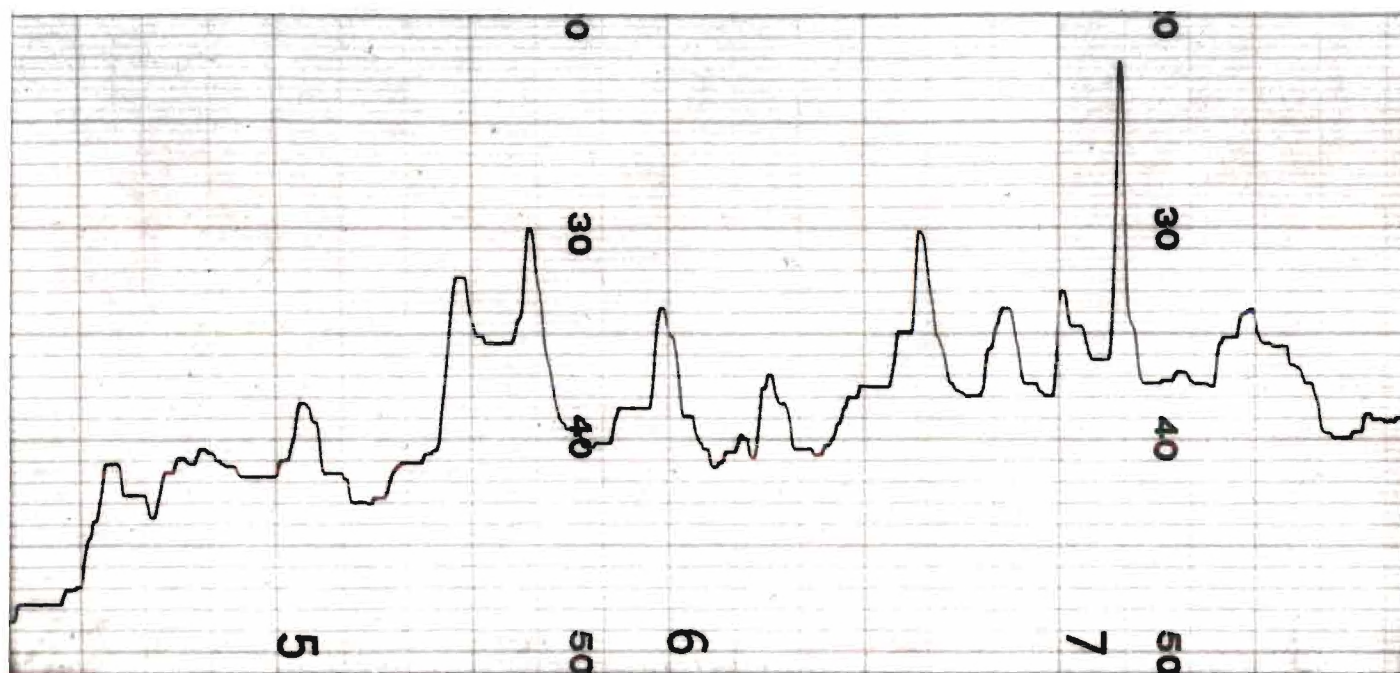


Figure 2. Microphotometer Trace of the Band
Near 6720 Å at 420 Gauss

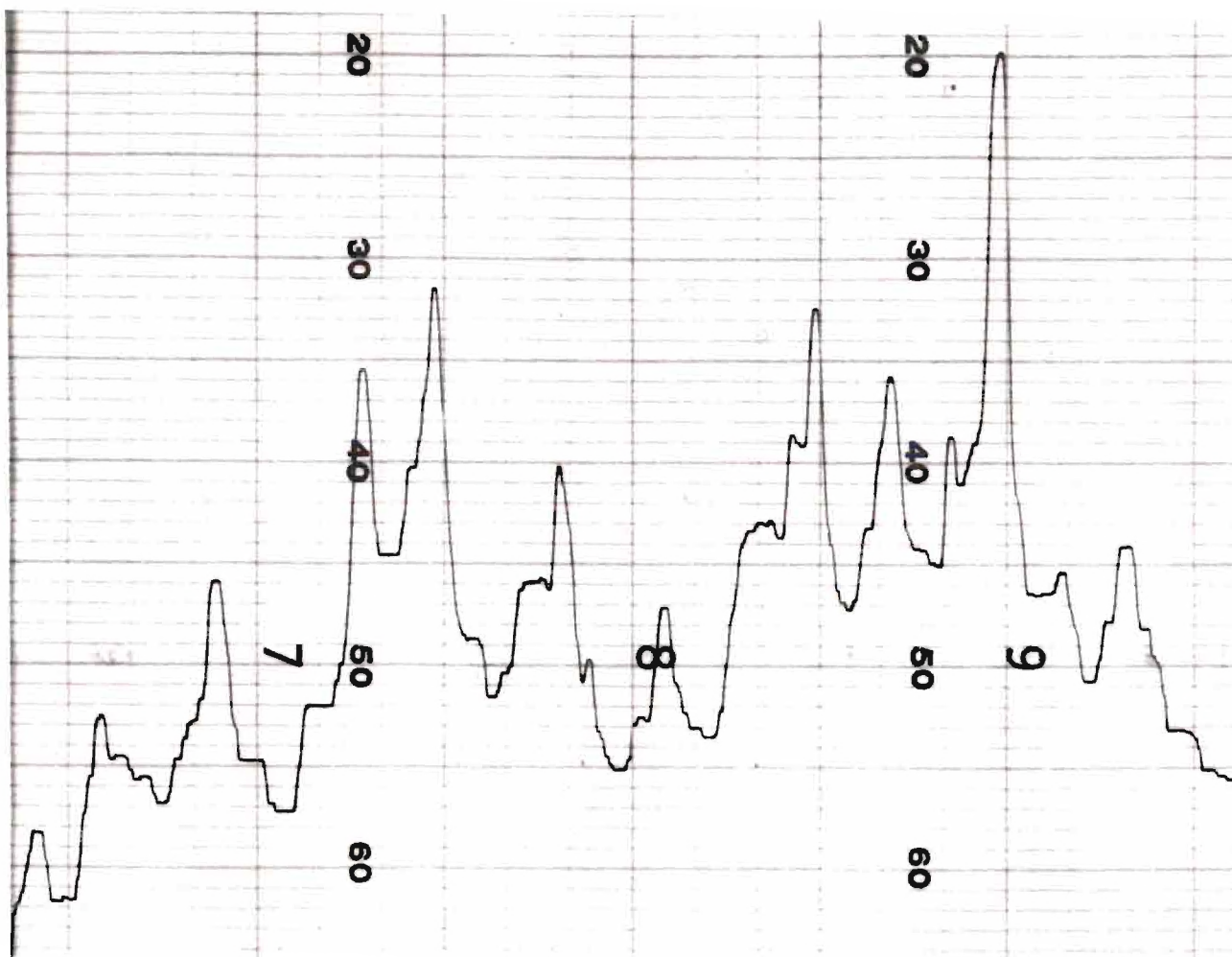


Figure 3. Microphotometer Trace of the Band
Near 6720 Å at 780 Gauss

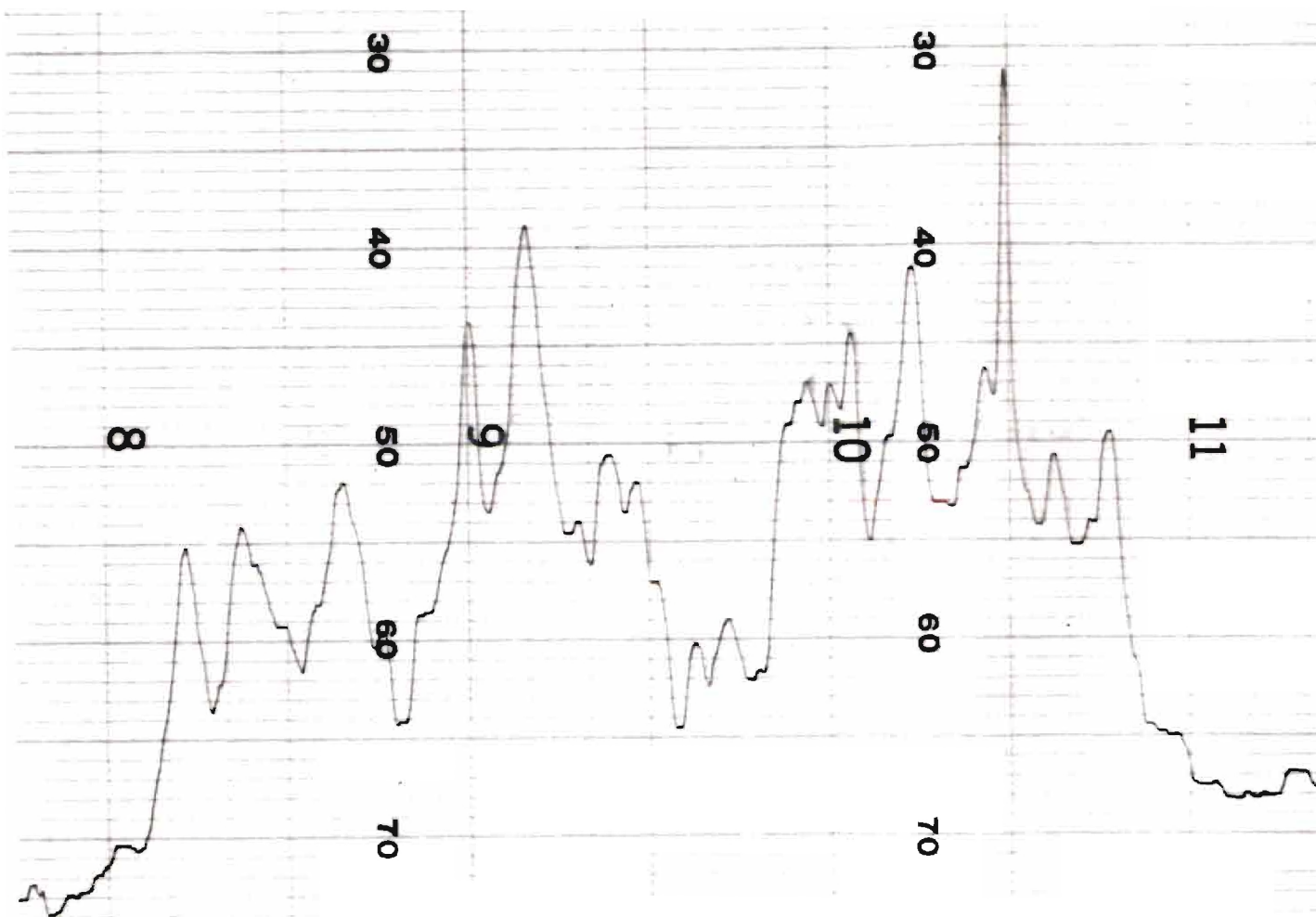


Figure 4. Microphotometer Trace of the Band
Near 6720 Å at 1350 Gauss

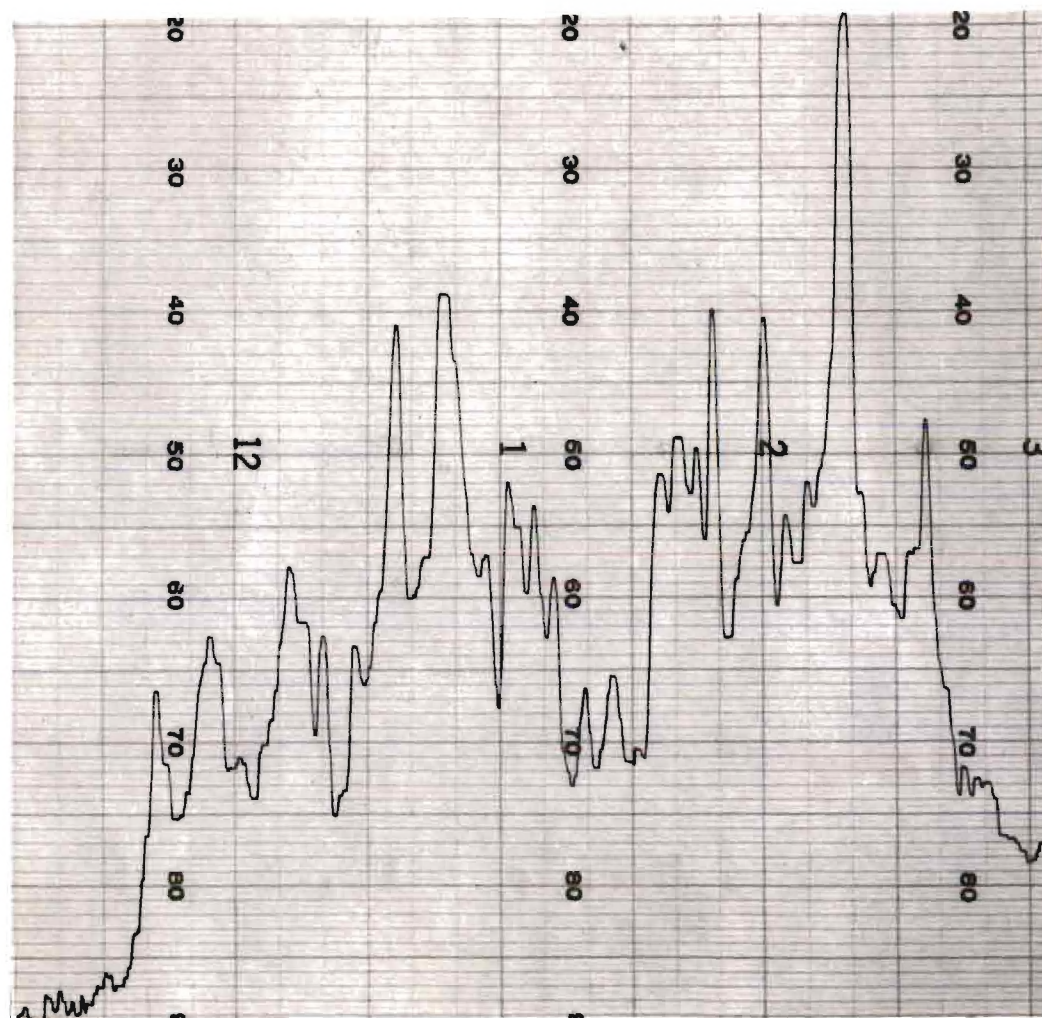


Figure 5. Microphotometer Trace of the Band
Near 6720 Å at 2000 Gauss

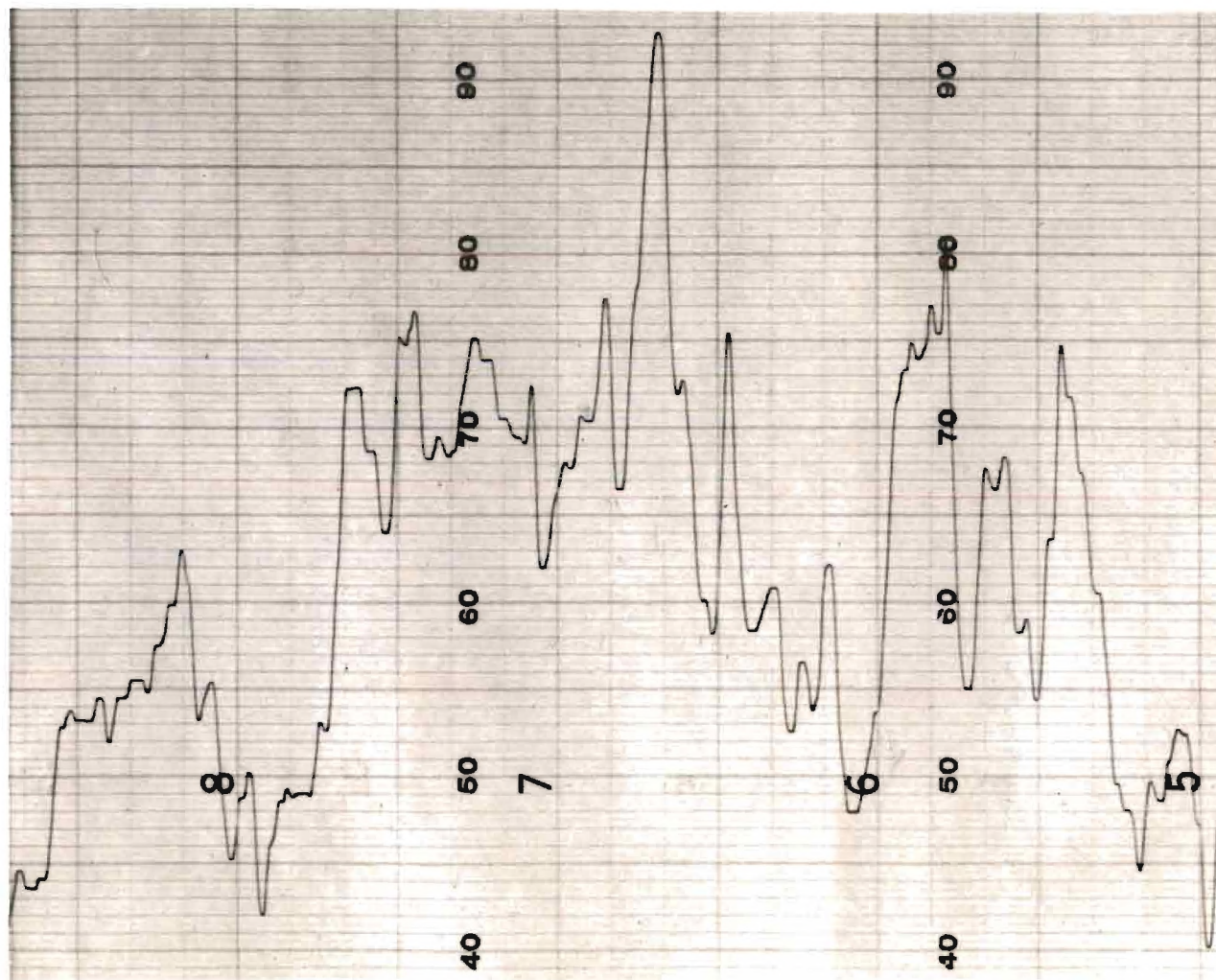


Figure 6. Microphotometer Trace of Absorption Spectrum
of Band Near 6720 Å

existence of a magnetic rotation spectrum depends upon the spin being coupled with the motion of the nuclear framework. If the spin is uncoupled by the field, the spectrum should disappear, with the possible exception of bands in which perturbations are involved. Coupling of this type would be expected to be weak, and relatively low fields would probably be sufficient to uncouple the spin. The electronic ground state of NO_2 is non-linear. Thus if the excited state of NO_2 which is responsible for the visible system were non-linear, the existence of the magnetic rotation spectrum would depend upon the type of coupling mentioned above. The extent of the magnetic rotation spectrum as well as its intensity make it extremely unlikely that the spectrum is a result of perturbations. Castle and Beringer (33), in a study of paramagnetic resonance in NO_2 , found that the electron spin is essentially free in a magnetic field of about 3000 gauss. Of the residual couplings, they found that spin-spin coupling with the nitrogen nucleus seems stronger than any other. It is reasonable to assume that a non-linear excited state would also experience a Paschen-Back effect at this field strength. Therefore, if the magnetic rotation spectrum in the visible system is due to a non-linear excited state, the spectrum should lose some intensity as the field strength is increased, because the spin will at least begin to uncouple, if indeed it does not uncouple completely. The observed behavior of the spectrum shows no intensity effect of this kind. In the ultraviolet

system of NO_2 a rotational analysis has been made by Harris and King (38) which indicates the excited state to be bent. Attempts by Herrmann (35) to find a magnetic rotation spectrum for this system were unsuccessful. Although the non-existence of a magnetic rotation spectrum for the ultraviolet system might conceivably be due to diffuseness of the bands, Harris and King assert that the bands in the vicinity of 2500 Å are very sharp. It seems likely that its non-existence in the ultraviolet system is due to a Paschen-Back effect. These arguments thus indicate that the excited state in the visible system must contain quantized electronic angular momentum other than spin. For this to be the case, the excited state must be linear so as to offer an axis upon which the component of electronic orbital angular momentum can be quantized. The most likely state is a 2Π state.

An attempt was made to arrange features into progressions. This attempt was not successful in that there was little correlation between the shapes of features in the progressions. Also only a few features in a band would belong to these progressions. It could not be concluded with any degree of confidence that features in a progression corresponded to analogous positions on consecutive bands. Nevertheless, intervals of approximately 650 cm^{-1} were found more frequently than other intervals. Although, because of the above mentioned difficulties, no real significance could be given to this interval, it is suggestive of a bending

vibrational frequency. Long "progressions" occur in the spectrum. This is consistent with the interpretation of the excited state as linear, because the Franck-Condon principle predicts long progressions in the bending vibration of the upper state for a transition in which there is a large change in angle.

The complexity of the spectrum can also be explained in terms of a linear excited state. A linear Y-X-Y molecule in which the degenerate bending mode of vibration is excited possesses vibrational angular momentum, quantized along the figure axis. This vibrational angular momentum is given by $\ell \frac{h}{2\pi}$, where ℓ may take the following values:

$$\ell = \pm V_2, \pm(V_2-2), \pm(V_2-4), \dots, \begin{cases} 1 \\ 0 \end{cases}. \quad (12)$$

V_2 is the vibrational quantum number giving the number of quanta of the degenerate bending vibration excited. In such a case an energy given by $g\ell^2$ must be added to the rotational energy. In an electronic transition in which the angle is changed significantly, it is chiefly the bending mode of vibration that is excited. Ramsay (51) has been able to give an analysis of the very complicated absorption spectrum of the NH_2 radical by making use of these facts. The spectrum of NH_2 extending from 4000 - 8300 Å was studied by Ramsay using a flash photolysis technique. Through a study of the isotope effect in N^{14}H_2 and N^{15}H_2 , he was able to assign the ground state to a bent configuration and the excited state to

a $^2\Pi$ state; he was able to explain the spacing of the features in terms of $g = 30 - 40 \text{ cm}^{-1}$. Vibrational assignments were made, and a small spin splitting was observed. Values for other parameters were also deduced. Although it is by no means as complicated a spectrum as that of NH_2 , the spectrum of the free HCO radical has been interpreted in a similar manner by Herzberg and Ramsay (52). For HCO a $^2\Sigma \leftarrow ^2A''$ transition was assigned with progressions exhibiting only even values of V'_2 . The authors assert that only states with $\ell = 0$ are important in the observed spectrum. NO_2 would be expected to be very similar to NH_2 , with different values for g and other parameters, however. Hydrides generally have small spin splittings, and the splitting in NO_2 would be expected to be much higher than in NH_2 , since in NO the splitting is about 121 cm^{-1} . Therefore, the complexity of the spectrum is easily accounted for.

The ground state of NO_2 is not really a symmetric top, since it does not have an axis of symmetry greater than a two-fold axis. Since two of the moments of inertia are much different from the third, NO_2 is however an "accidental" symmetric top. It is sufficiently close to being a symmetric top to account for the infrared spectrum (28) and the rotational structure of the ultraviolet system (38). The unique axis of the top is a line in the plane of the molecule, perpendicular to the two-fold axis. Upon this axis the projection, $K \frac{h}{2\pi}$, of the total angular momentum, $\sqrt{J(J+1)} \frac{h}{2\pi}$,

is nearly quantized. The rotational energy levels depend upon the values of K and J in the following way:

$$F''(J,K) = J(J+1)B'' + K'^2(A''-B'').$$

If the excited state is also a symmetric top, the rotational structure of the spectrum is determined by certain selection rules:

$$\Delta J = \pm 1, 0; \Delta K = \pm 1 \text{ or } \Delta K = 0. \quad (13)$$

Of the structures due to J and K , that due to K is more coarse and is probably the more important as far as structure resolved in this investigation is concerned. $\Delta K = \pm 1$ holds when the electronic transition is such that the electric vector vibrates in a plane perpendicular to the unique axis of the top. $\Delta K = 0$ holds when the transition is such that the electric vector vibrates in a plane parallel to the unique axis. It is possible in cases where the top is not really a symmetric top that both perpendicular and parallel transitions may occur.

A linear molecule with electronic and vibrational angular momenta is a symmetric top, the unique axis being the figure axis of the molecule. We will define an effective $K' = \Lambda + \ell$ and leave the spin to manifest itself as a splitting. The rotational energy levels of such a molecule may be written:

$$F'(J, \Lambda, \ell) = J(J+1)B' + (A'-B')\Lambda^2 + g\ell^2. \quad (14)$$

Since Λ is constant in the transition, the term containing Λ may be ignored in considering the spacings in a band. If the excited state of NO_2 is indeed a $^2\Pi$ state, then $\Lambda = 1$.^{*} In Tables 3 and 4 the possible transitions to be expected in both the perpendicular and parallel cases are tabulated for a number of values of V_2' . The position of a sub-band is determined by $|K''|$ and $|\ell|$. The number of sub-bands in a band, ignoring the spin splitting for the moment, is equal to the number of distinct pairs of $|K''|$ and $|\ell|$. Thus, as the value of V_2' goes down in a progression the bands should become simpler, because the possible number of ℓ values decreases. Of course the spin splitting will double everything, but the tendency toward simplicity should be marked. This is observed to be the case in the magnetic rotation spectrum. Moving toward longer wave-lengths the bands become simpler, and the simplest band observed is the last one developed. The fact that only a relatively small number of sub-bands are to be expected, because of the restrictions on the number of ℓ values, explains the somewhat abrupt breaking-off of structure in the bands. Previous attempts to attribute the phenomenon to head formation for a non-linear excited state were unsuccessful because the features converged much too slowly. Similarly, on the other side of the band, the

^{*}Strictly speaking -1 should be considered as well as $+1$, but its consideration yields no results not already contained in the results found from the $+1$ value. Thus in this discussion only the positive value is used.

Table 3. Quantum Numbers for Allowed Transitions

V'_2	ℓ	Λ	K'	$\Delta K = +1$ K''	$\Delta K = -1$ K''	$\Delta K = 0$ K''
0	0	1	1	0	2	1
1	1	1	2	1	3	2
1	-1	1	0	-1	1	0
2	2	1	3	2	4	3
2	0	1	1	0	2	1
2	-2	1	-1	-2	0	-1
3	3	1	4	3	5	4
3	1	1	2	1	3	2
3	-1	1	0	-1	1	0
3	-3	1	-2	-3	-1	-2
4	4	1	5	4	6	5
4	2	1	3	2	4	3
4	0	1	1	0	2	1
4	-2	1	-1	-2	0	-1
4	-4	1	-3	-4	-2	-3
5	5	1	6	5	7	6
5	3	1	4	3	5	4
5	1	1	2	1	3	2
5	-1	1	0	-1	1	0
5	-3	1	-2	-3	-1	-2
5	-5	1	-4	-5	-3	-4
6	6	1	7	6	8	7
6	4	1	5	4	6	5
6	2	1	3	2	4	3
6	0	1	1	0	2	1
6	-2	1	-1	-2	0	-1
6	-4	1	-3	-4	-2	-3
6	-6	1	-5	-6	-4	-5
7	7	1	8	7	9	8
7	5	1	6	5	7	6
7	3	1	4	3	5	4
7	1	1	2	1	3	2
7	-1	1	0	-1	1	0
7	-3	1	-2	-3	-1	-2
7	-5	1	-4	-5	-3	-4
7	-7	1	-6	-7	-5	-6
8	8	1	9	8	10	9
8	6	1	7	6	8	7
8	4	1	5	4	6	5

Table 3. (Concluded)

V_2'	l	Λ	K'	$\Delta K = +1$ K''	$\Delta K = -1$ K''	$\Delta K = 0$ K''
8	2	1	3	2	4	3
8	0	1	1	0	2	1
8	-2	1	-1	-2	0	-1
8	-4	1	-3	-4	-2	-3
8	-6	1	-5	-6	-4	-5
8	-8	1	-7	-8	-6	-7
9	9	1	10	9	11	10
9	7	1	8	7	9	8
9	5	1	6	5	7	6
9	3	1	4	3	5	4
9	1	1	2	1	3	2
9	-1	1	0	-1	1	0
9	-3	1	-2	-3	-1	-2
9	-5	1	-4	-5	-3	-4
9	-7	1	-6	-7	-5	-6
9	-9	1	-8	-9	-7	-8

Table 4. Number and Characterizations of Sub-bands for Various Values of V_2'

V_2'	$\Delta K = \pm 1$			$\Delta K = 0$		
	$ L $	$ K'' $	No. of Sub-bands	$ L $	$ K'' $	No. of Sub-bands
0	0	0	2	0	1	1
1	0	2				
1	1	1	2	1	2	2
	1	3		1	0	
2	2	2	5	2	3	3
	0	0		0	1	
	2	0		2	1	
	0	2				
	2	4				
3	3	3	5	3	4	4
	1	1		1	2	
	3	1		1	0	
	1	3		3	2	
4	3	5				
4	4	4	8	4	5	5
	2	2		2	3	
	0	0		0	1	
	2	0		2	1	
	0	2		4	3	
	2	4				
	4	6				
5	4	2				
5	5	5	8	5	6	6
	3	3		3	4	
	1	1		1	2	
	3	1		1	0	
	1	3		3	2	
	3	5		5	4	
	5	7				
6	5	3				
6	6	6	11	6	7	7
	4	4		4	5	
	2	2		2	3	
	0	0		0	1	
	6	4		2	1	
	4	2		4	3	
	2	0		6	5	
	0	2				

Table 4. (Concluded)

V_2'	$\Delta K = \pm 1$			$\Delta K = 0$		
	$ L $	$ K'' $	No. of Sub-bands	$ L $	$ K'' $	No. of Sub-bands
6	2	4	11			8
	4	6				
	6	8				
7	7	7		7	8	
	5	5		5	6	
	3	3		3	4	
	1	1		1	2	
	7	9		1	0	
	5	7		3	2	
	3	5		5	4	
	1	3		7	6	
	3	1	14			9
	5	3				
	7	5				
8	8	8		8	9	
	6	6		6	7	
	4	4		4	5	
	2	2		2	3	
	0	0		0	1	
	8	10		2	1	
	6	8		4	3	
	4	6		6	5	
	2	4		8	7	
	0	2				
	2	0				
	4	2				
	6	4				
	8	6	14			10
9	9	9		9	10	
	7	7		7	8	
	5	5		5	6	
	3	3		3	4	
	1	1		1	2	
	9	11		1	0	
	7	9		3	2	
	5	7		5	4	
	3	5		7	6	
	1	3		9	8	
	3	1				
	5	3				
	7	5				
	9	7				

abrupt breaking-off of the band was too sharp to be attributed to a decreasing Boltzmann factor. These aspects of the band structure lend strong support to the assumption of a linear excited state.

Since the bands on the red end of the observed magnetic rotation spectrum are the simplest, these bands were selected for analysis. In order of decreasing wave-length these bands are labelled the 7410 Å, the 7090 Å, and the 6720 Å bands. The wave-length used as the label for a band represents a wave-length approximately in the middle of the group of features. Bands increase in complexity rapidly in the direction of shorter wave-lengths. The precision of wave number differences between features also goes down with a decrease in wave-length. In the analysis of these bands the assumption is made that the positions of features represent the positions of sub-bands due to the K structure of the spectrum. An analysis should yield the value of g ; the spin splitting; assignments of Q , K , and V_2' ; and a decision as to whether the transition is parallel, perpendicular, or hybrid. A necessary but not a sufficient condition for a good analysis is that the assignment must yield a value of $(A''-B'')$ which is close to the value obtained from infrared work, 7.62 cm^{-1} .

A microphotometer trace of the 7410 Å band is given in Figure 7. In Table 5 the wave-lengths and wave number values of the numbered features are given. The feature marked A is an argon line at 7384 Å. Table 6 contains wave number

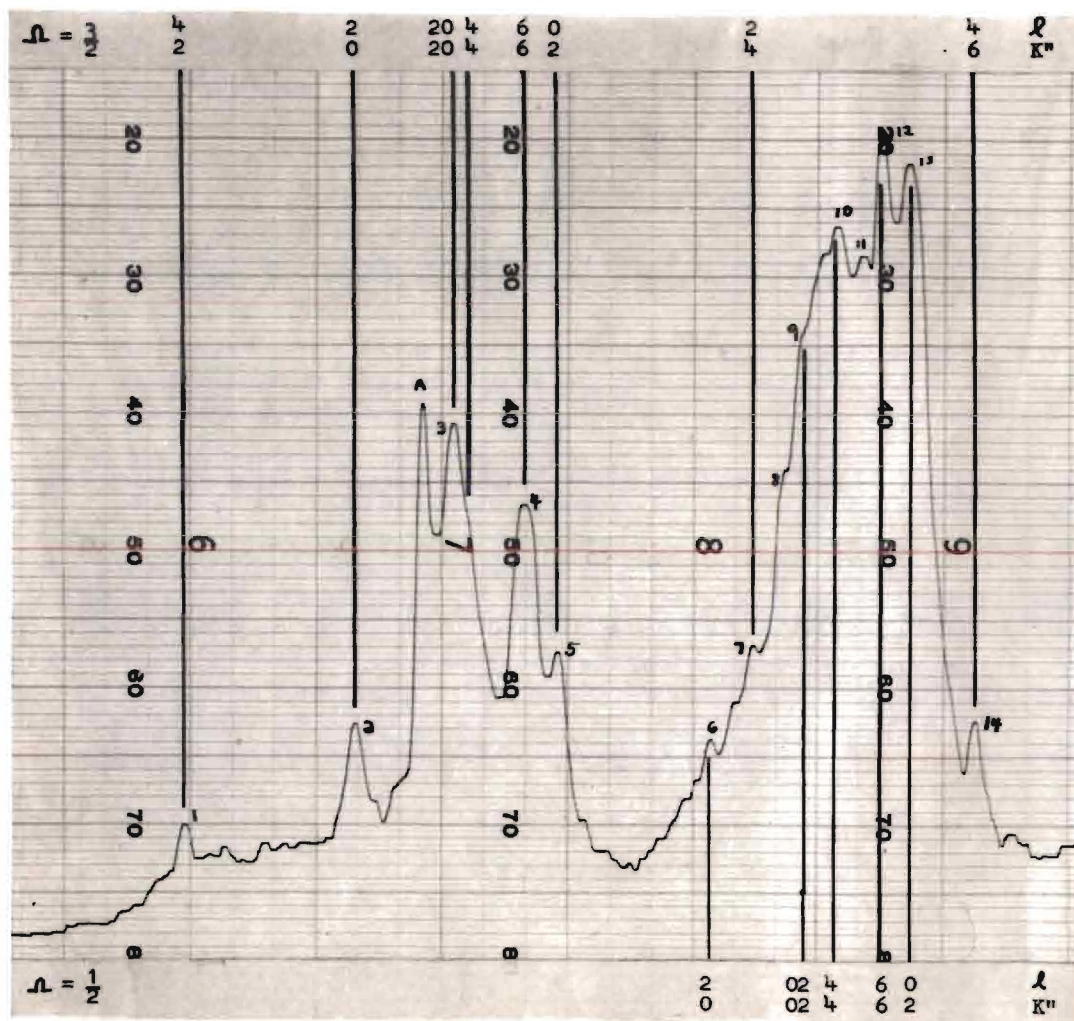


Figure 7. Microphotometer Trace and Assignments
for the 7410 A Band

Table 5. Wave-lengths and Frequencies of Features in
the 7410 Å Band

Feature No.	Wave-length Å	Frequency cm ⁻¹
1	7344	13613
2	7373	13559
3	7389	13530
4	7399	13512
5	7406	13499
6	7431	13453
7	7438	13441
8	7444	13430
9	7447	13425
10	7452	13416
11	7456	13408
12	7460	13401
13	7464	13394
14	7475	13374

Data taken from film no. 109.

Slit width: 0.2 mm.

Field strength: approximately 1800 gauss.

Table 6. Wave Number Differences Between Features in the 7410 A Band

	1	2	3	4	5	6	7	8	9	10	11	12	13	14
1	0													
2	54	0												
3	83	29	0											
4	101	47	18	0										
5	114	60	31	13	0									
6	160	106	77	59	46	0								
7	172	118	89	71	58	12	0							
8	183	129	100	82	69	23	11	0						
9	188	134	105	87	74	28	16	5	0					
10	197	143	114	96	83	37	25	14	9	0				
11	205	151	122	104	91	45	33	22	17	8	0			
12	212	158	129	111	98	52	40	29	24	15	7	0		
13	219	165	136	118	105	59	47	36	31	22	14	7	0	
14	239	185	156	138	125	79	67	56	51	42	34	27	20	0

differences between the features. The position of a sub-band relative to the band origin is determined by:

$$g\ell^2 - K''^2(A''-B''). \quad (15)$$

Therefore the spacing is determined by the values of g and $(A''-B'')$. Plots were constructed which give the spacings of sub-bands for different values of g . In these plots values of g are plotted as ordinates, and the abscissa is $-K''^2(A''-B'')$. For convenience in construction, $(A''-B'')$ was set equal to 10 units. To use these plots the positions of the features in wave numbers were marked on a piece of paper, using the same scale as the plots. The piece of paper was moved up and down until spacings on the paper coincided with spacings on the plot. Such a coincidence corresponds to an assignment of ℓ and K'' values to features and fixes the value of g as well. Figures 8, 9, 10, and 11 are plots of the kind described above, representing both perpendicular and parallel transitions and even and odd values of V_2' . The best fit for the 7410 Å band was found to indicate a perpendicular transition with $V_2' = 6$. The assignment of features to ℓ and K'' values is shown in Figure 7. Each part of the spin multiplet is labelled by its value of $\mathcal{N} = \Lambda + \Sigma$. A good fit could not be obtained for odd values of V_2' and a perpendicular transition, nor could it be obtained for even and odd values of V_2' in the case of a parallel transition. Using the assignment found in this way, the value of g obtained is $6.9 \pm 0.1 \text{ cm}^{-1}$,

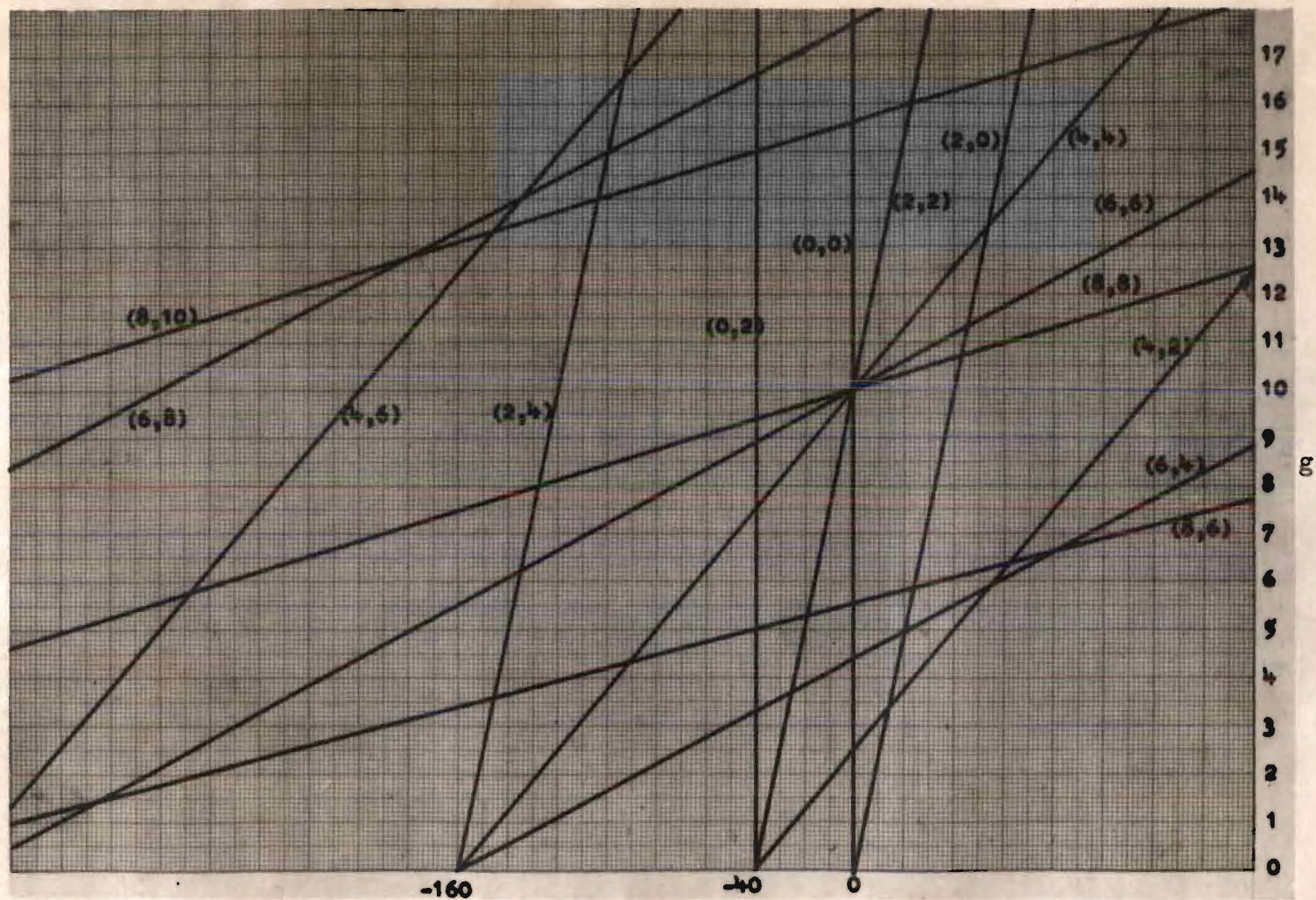


Figure 8. Spacing versus g for a Perpendicular Transition and $V_2' = 8$

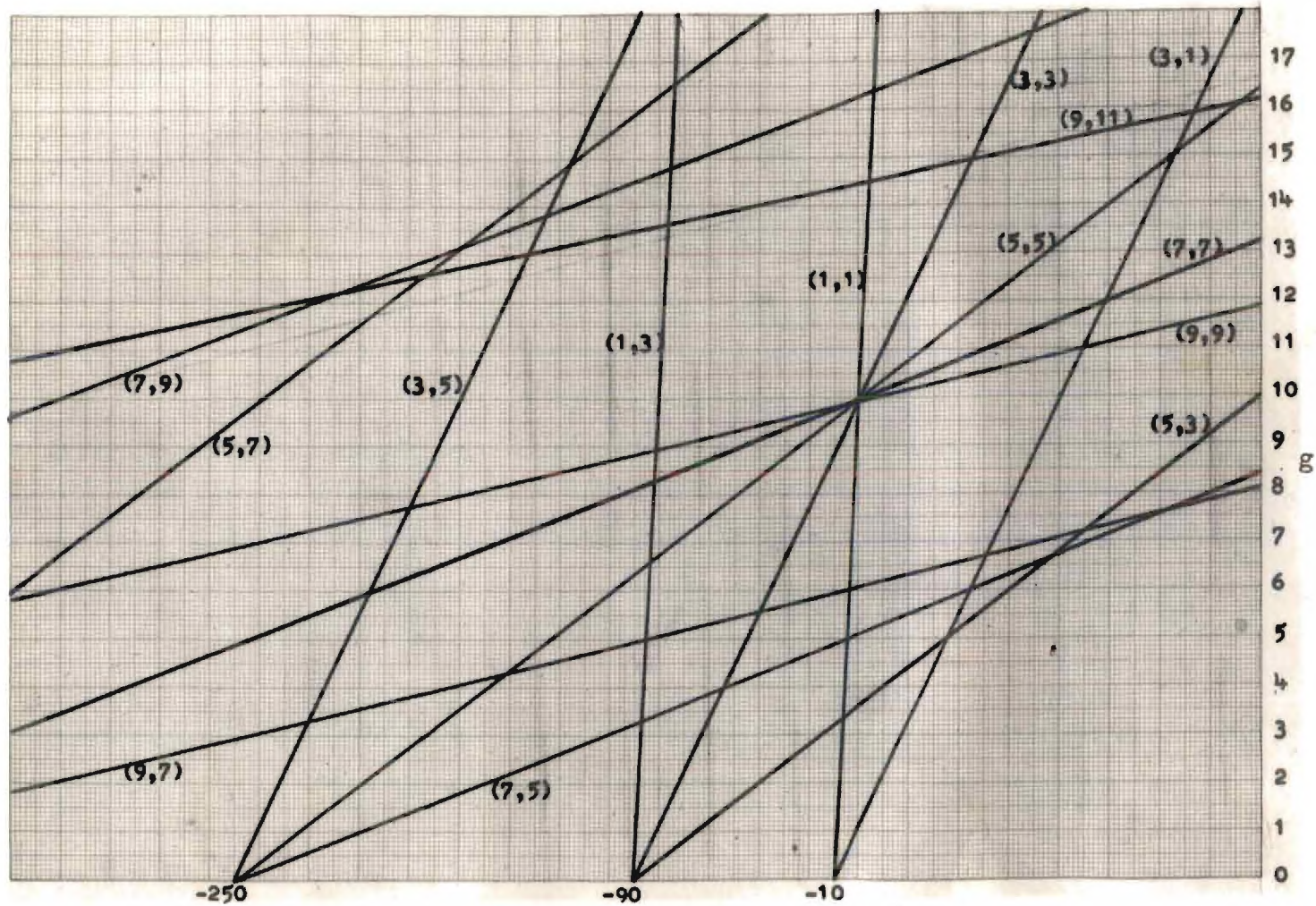


Figure 9. Spacing versus g for a Perpendicular Transition and $V'_2 = 9$

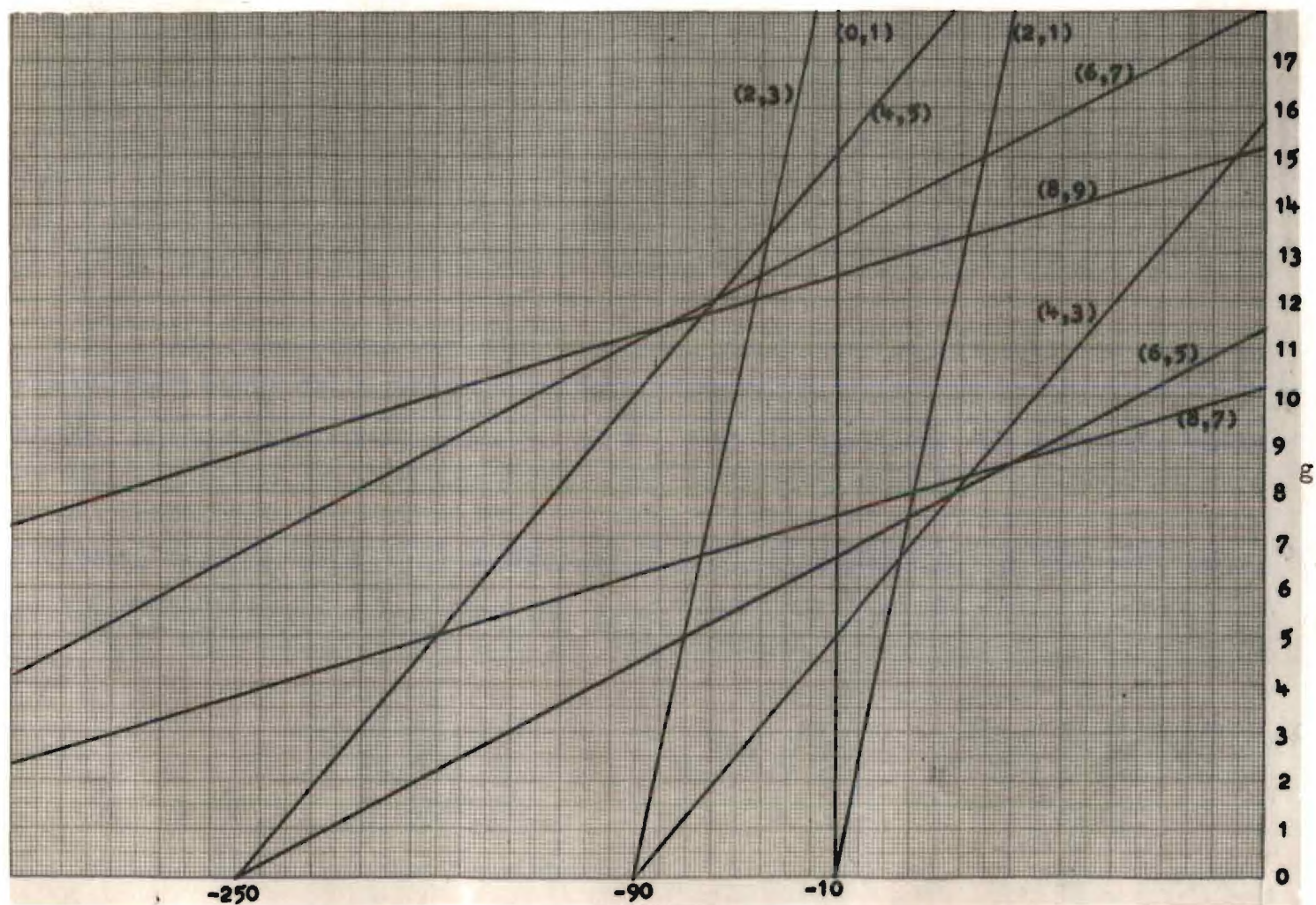


Figure 10. Spacing versus g for a Parallel Transition and $V_2' = 8$

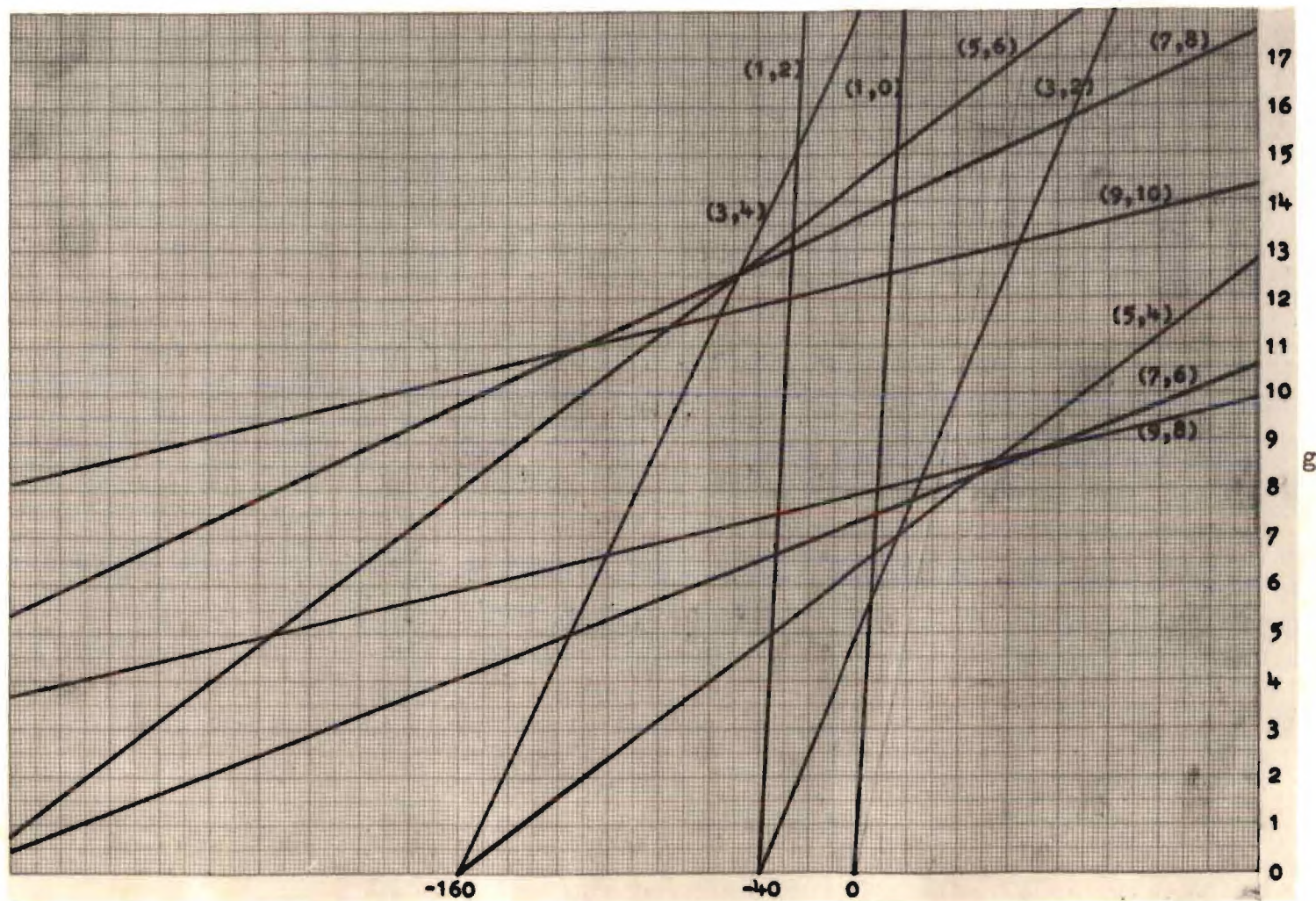


Figure 11. Spacing versus g for a Parallel Transition and $V_2^1 = 9$

and the value of $(A''-B'')$ obtained is $7.4 \pm 0.1 \text{ cm}^{-1}$. The value 7.4 cm^{-1} is in good agreement with the value found from infrared work, 7.62 cm^{-1} . The spin splitting resulting from the assignment is approximately 107 cm^{-1} . It will be shown later that the spin splitting depends upon V_2' . Features numbered 8 and 11 are unassigned. A critical examination of assignments will be given later. Some of the less significant features and suggestions of features can be interpreted as arising from parallel sub-bands.

The 7090 A band will be discussed after the 6720 A band because of a difficulty in the assignment. The 6720 A band is the band whose variation with magnetic field intensity has been shown in Figures 2, 3, 4, and 5. It will be noticed that the trace of the spectrum taken at the lowest field used shows the simplest structure. Thus, although the other bands were analyzed at moderately strong fields, an analysis of the 6720 A band was attempted at a low field. The method of analysis was the same as that used for the 7410 A band. Table 7 contains a list of the wave-lengths of frequencies of the numbered features, and Table 8 contains wave number differences for these features. The assignment of ℓ and K'' values is given in Figure 12. From the assignment given in the figure, the value of g was found to be $6.8 \pm 0.1 \text{ cm}^{-1}$, and the value of $(A''-B'')$ was found to be $7.4 \pm 0.1 \text{ cm}^{-1}$. Both of these values are in good agreement with those obtained from the assignment of the 7410 A band. A different spin

Table 8. Wave Number Differences Between Features in the 6720 A Band

	1	2	3	4	5	6	7	8	9	10	11	12	13
1	0												
2	14	0											
3	39	25	0										
4	52	38	13	0									
5	69	55	30	17	0								
6	82	68	43	30	13	0							
7	100	86	61	48	31	18	0						
8	122	108	83	70	53	40	22	0					
9	150	136	111	98	81	68	50	28	0				
10	166	152	127	114	97	84	66	44	16	0			
11	198	184	159	146	129	116	98	76	48	32	0		
12	218	204	179	166	149	136	118	96	68	52	20	0	
13	237	223	198	185	168	155	137	115	87	71	39	19	0

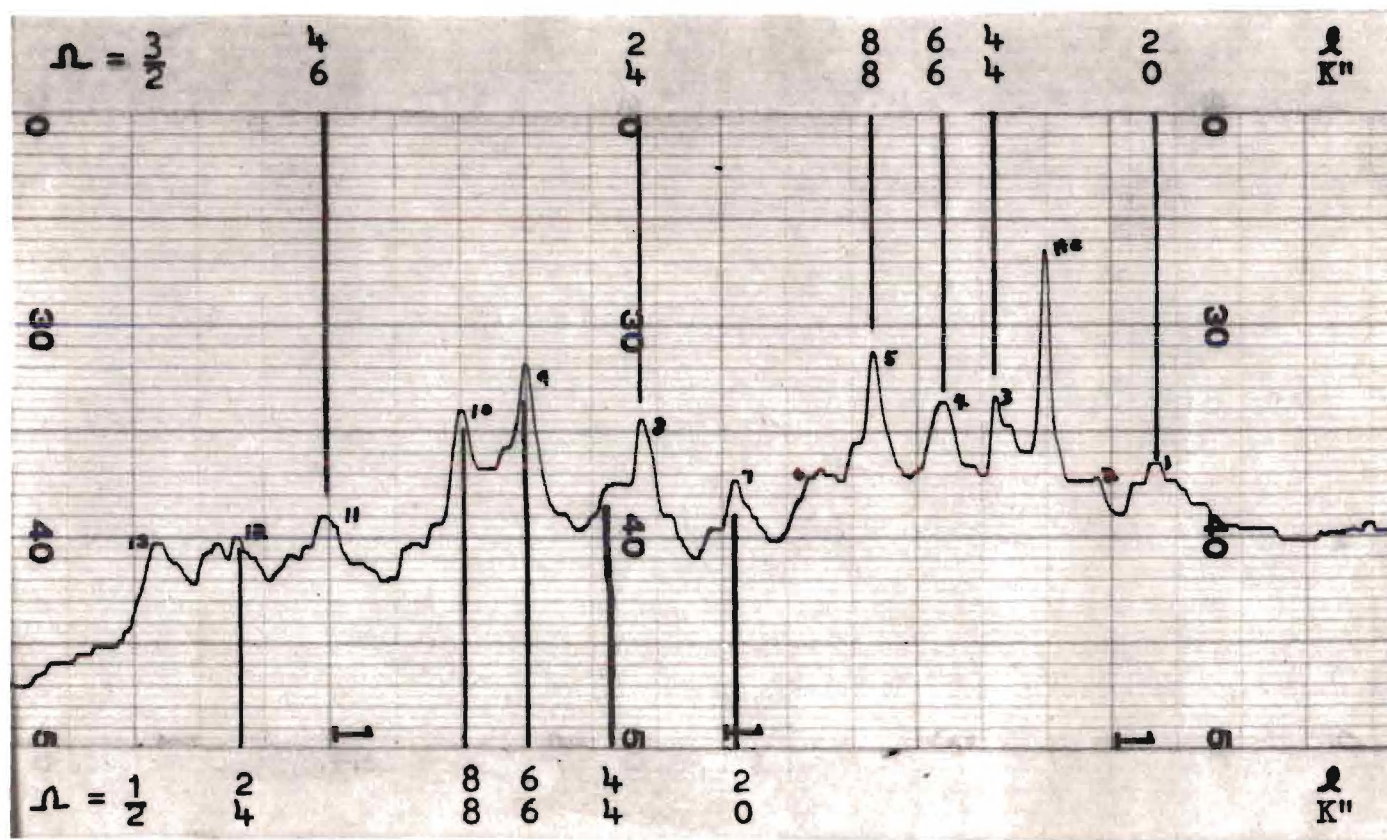


Figure 12. Microphotometer Trace and Assignments for the 6720 Å Band

splitting was obtained however. Its value was found to be approximately 98 cm^{-1} rather than 107 cm^{-1} . This is not surprising since, as the molecule vibrates more and more, Λ loses some of its significance. The interaction between Λ and the spin would thus be expected to decrease with an increase in V_2' , hence the lower spin splitting. Features 2, 6, and 13 are unassigned. Here again some of the minor features correspond to the calculated positions of parallel sub-bands.

The 7090 A band was approached in the same manner as the 7410 A and 6720 A bands. The assignment for this band is not as satisfactory as those for the 7410 A and 6720 A bands. The best fit was found in the case of a perpendicular transition. At first it seemed that $V_2' = 9$ was indicated. An argument might be made for attributing the 6720 A band to $V_2' = 10$, but there would be difficulty in that the 7410 A band could not be fitted into this scheme. Therefore, it is assumed that the 7090 A band belongs to $V_2' = 7$. Wave-lengths and frequencies and wave number differences for the numbered features are given in Tables 9 and 10 respectively. Using the assignment shown in Figure 13, values for g and $(A''-B'')$ were calculated. Only the values of g and $(A''-B'')$ obtained by using features 2, 3, and 10 were consistent with the values obtained from the 7410 A and 6720 A bands. The values found by using features 2, 3, and 10 were 7.0 cm^{-1} for g and 7.6 cm^{-1} for $(A''-B'')$. Values of $(A''-B'')$ calculated using

Table 10. Wave Number Differences Between Features in the 7090 A Band

	1	2	3	4	5	6	7	8	9	10
1	0									
2	10	0								
3	25	15	0							
4	43	33	18	0						
5	67	57	42	24	0					
6	75	65	50	32	8	0				
7	136	126	111	93	69	61	0			
8	166	156	141	123	99	91	30	0		
9	189	179	164	146	122	114	53	23	0	
10	193	183	168	150	126	118	57	27	4	0

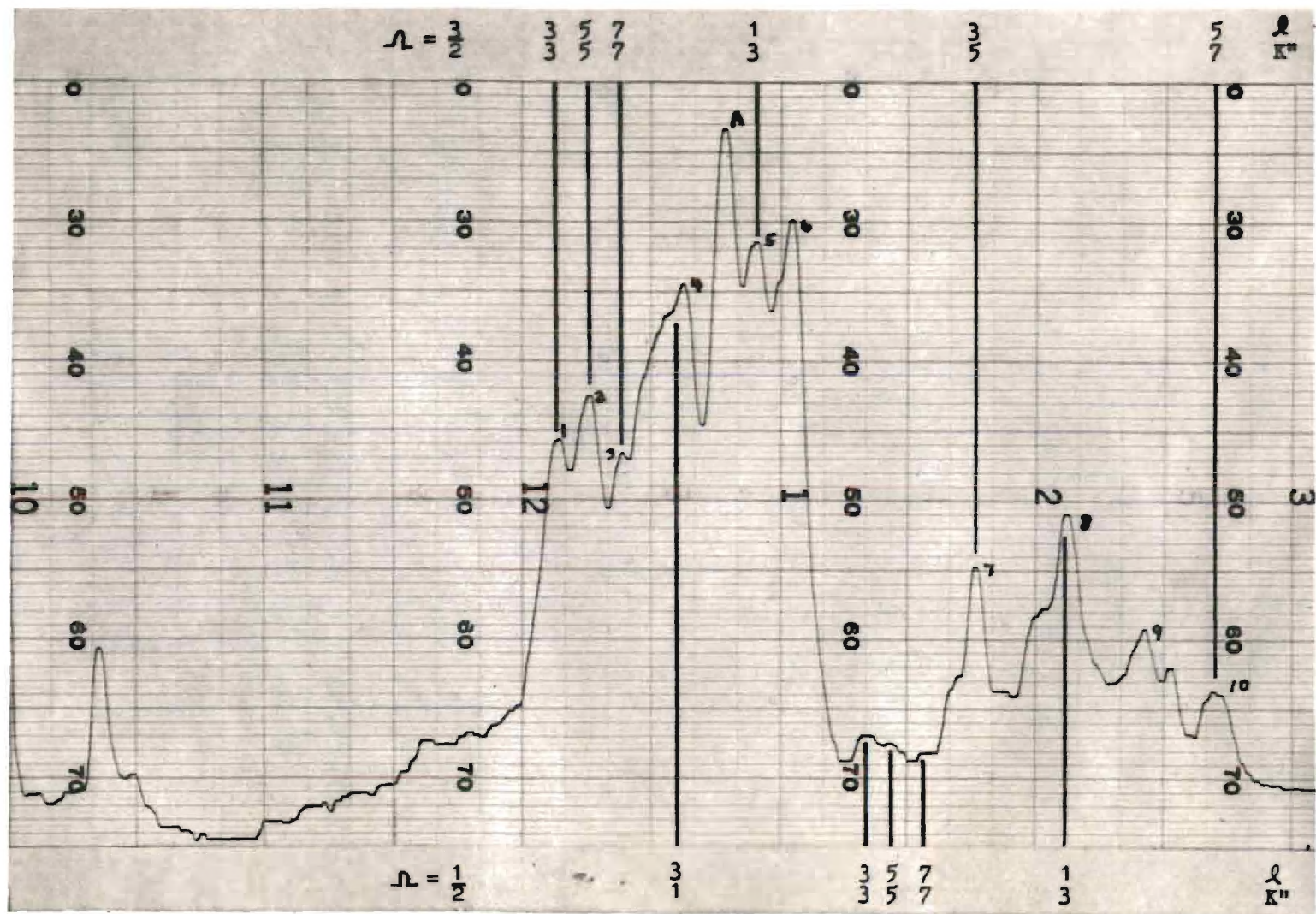


Figure 13. Microphotometer Trace and Assignments for the 7090 Å Band

other features ranged from 6.9 cm^{-1} to 9.0 cm^{-1} . There is something anomalous about the band also, in that most features in the part of the spin doublet in which $\Omega = \frac{1}{2}$ are either completely absent or are of very low intensity. The number of major features which are unassigned is also greater than in the other bands. If features 5 and 8 are correctly assigned, the spin splitting is about 99 cm^{-1} . This value is consistent with the trend noticed in the 7410 Å and 6720 Å bands.

In order to find the vibrational interval between the bands, the position of the band origin was calculated for one part of the spin doublet in each band. The spin splitting was then used to find the origin of the hypothetical unsplit band. By taking differences between the frequencies of these origins the following approximate intervals were obtained:

The 7410 Å, 7090 Å band interval = 653 cm^{-1} .

The 7090 Å, 6720 Å band interval = 769 cm^{-1} .

One-half the 7410 Å, 6720 Å band interval = 711 cm^{-1} .

The large difference between the 7410 Å, 7090 Å band interval and the 7090 Å, 6720 Å band interval coupled with the irregular behavior of the features of the 7090 Å band suggest that the 7090 Å band is perturbed by Fermi resonance. If it is assumed that the 7410 Å and 6720 Å bands are unperturbed, the vibrational frequency for the bending mode would be expected to be in the neighborhood of 710 cm^{-1} . This value of ν_2' would indicate the origin of the system to be at about 9220 cm^{-1} or 10800 Å.

It is interesting to compare the results given above with predictions derived from some theoretical calculations. The symmetries and ordering of the electronic states of AB_2 molecules have been discussed by Mulliken (53), Walsh (54), and Trawick (1). Mulliken and Walsh both give correlation diagrams showing the order of energy levels as a function of bond angle. Walsh's correlation diagram is shown in Figure 14. The curves correlate states of a bent molecule with states of a linear molecule. The direction and steepness of descent of the curves give a measure of how the occupancy of orbitals by electrons affects the bond angle. Walsh points out that the shapes of AB_2 , non-hydride molecules in their ground states are easily explained using the diagram. NO_2 has 17 valence electrons, the 17th electron going into the a'_1 orbital. This would make the ground state a 2A_1 state with the odd electron in a non-bonding orbital localized on the nitrogen atom, which is the same result that is obtained experimentally from microwave studies (32). Chemical evidence for the localization of the odd electron on the nitrogen atom lies in the fact that NO_2 behaves as a nitro group radical. The most likely excited states for the visible system (in C_{2v} notation) are the A_1 and B_1 states, obtained by elevating the electron in the a'_1 state to the \bar{a}''_1 and b''_1 states respectively. Both of these possible transitions would lead to an excited state in which the bond angle is much larger than in the ground state, since in both the electron is

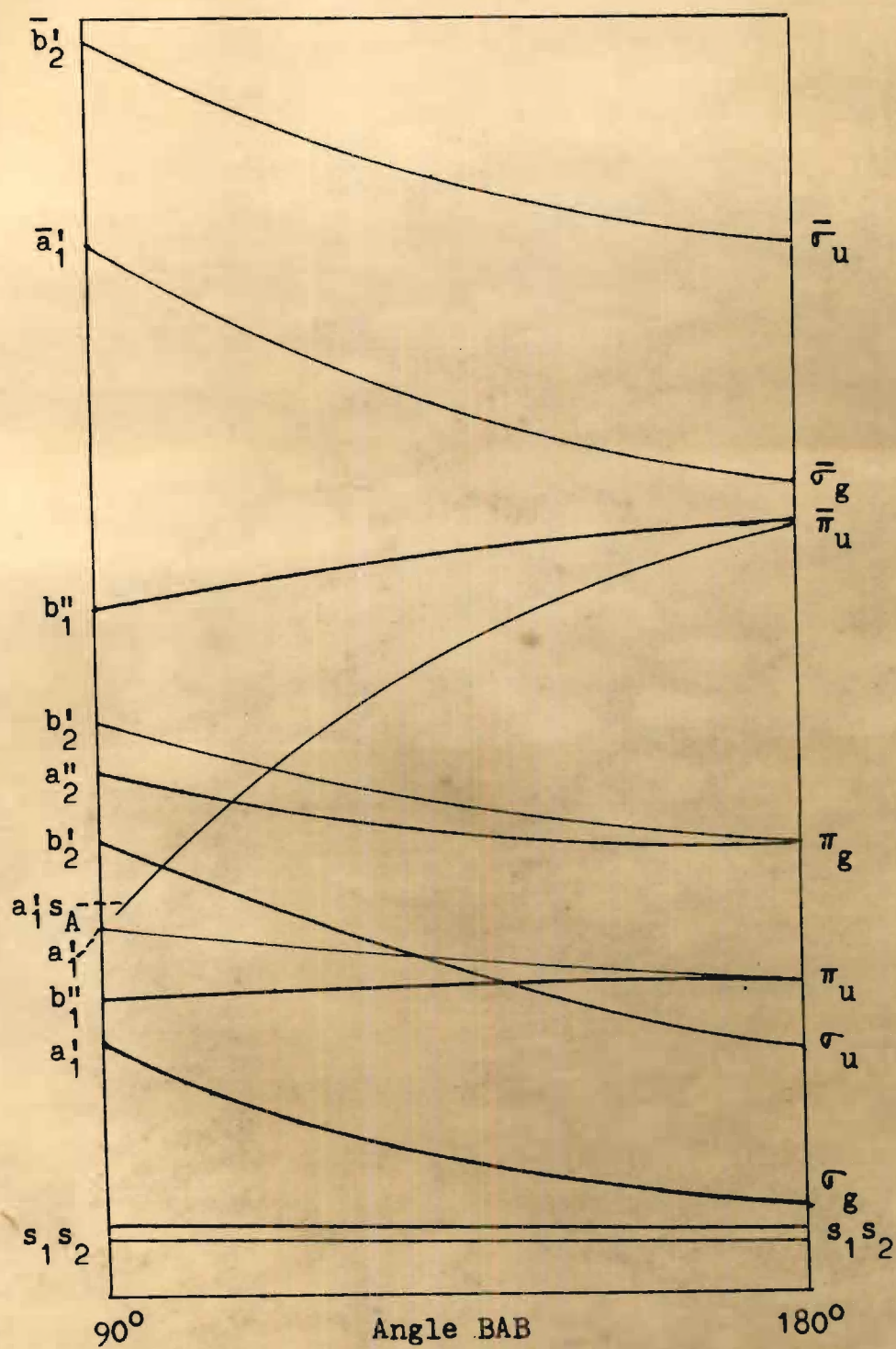


Figure 14. Walsh's Correlation Diagram

removed from the a_1' orbital which slopes strongly to the left. The ground state of NO_2^+ in which there is no electron in this orbital has been reported to be linear (55). Thus both of these transitions could easily lead to a linear excited state. For reasons already discussed, the excited state is assigned to a ${}^2\pi$ state. An examination of the correlation diagram shows that a transition to the b_1'' orbital would indeed lead to a π state, whereas a transition to the \bar{a}_1'' state would lead to a Σ state. Since the Franck-Condon principle requires that there be no change in nuclear configuration at the instant of the transition, readjustment being made later, the perpendicular or parallel nature of the transition is determined by the C_{2v} excited state. In the case of the transition to the b_1'' orbital, the C_{2v} excited state would be a B_1 state. This fact requires that the transition be perpendicular.¹ Therefore the results obtained in this investigation are entirely consistent with the interpretation that the spectrum is due to an $a_1' \rightarrow b_1''$ transition. It is encouraging that Trawick deduced exactly the same transition for the corresponding system in the nitrite ion, as a result of studies of the polarized ultraviolet spectra of nitrite crystals at low temperature. In Trawick's notation the transition is designated by $n_N \rightarrow \pi^*$.

For the sake of completeness some of the difficulties

¹A more detailed discussion of this point is found in the appendix.

in the analysis of the bands must be mentioned. In the bands analyzed there are some unassigned bands. Even more of a problem is the existence of the magnetic field effect in which there is an appearance of features with an increase in field. This effect has not been explained. It must also be recalled that the assumption was made that all features represented sub-bands in the K structure. This assumption ignores the possibility that separations between P and Q branches may possibly be large enough to lead to two features instead of one. In spite of these facts the analysis seems reasonable and consistent.

CHAPTER VII

CONCLUSIONS AND RECOMMENDATIONS

Conclusions.--The excited electronic state of the visible system of NO_2 is concluded to be linear in a ${}^2\Pi$ state. The transition is assigned to a ${}^2\Pi \leftarrow {}^2A_1$ transition in which an electron is elevated from a non-bonding orbital localized on the nitrogen atom to an anti-bonding π orbital. In the ground state the molecule is an accidental symmetric top, and in the excited state it is a true symmetric top. It was found that in the transition the electric vector vibrates in a plane perpendicular to the unique axis of the top.

The complexity of the spectrum is ascribed to the existence of vibrational angular momentum, quantized about the figure axis of the excited state in addition to electronic angular momentum. This vibrational angular momentum, $\ell \frac{h}{2\pi}$, is due to the degenerate bending vibration which is excited in long progressions as a consequence of the Franck-Condon principle. Spacing of features in the bands is determined by an effective $K = \Lambda + \ell$ and the selection rule, $\Delta K = \pm 1$. Of course, $\Lambda = 1$ for a Π state. The position of a sub-band with respect to the zero position is determined by a term of the form $g\ell^2$. The number of sub-bands is fixed by the value of V_2' . Assignments were made for bands at 7410 Å, 7090 Å, and 6720 Å. Values for $(A''-B'')$, g , and the spin splitting

were obtained. These results are tabulated in Table 11.

Table 11. Parameters Resulting from Band Assignments

Band A	(A"-B") cm ⁻¹	g cm ⁻¹	Spin Splitting cm ⁻¹	Est. Origin cm ⁻¹	Interval cm ⁻¹	V ₂ ¹
7410	7.4 ± 0.1	6.9 ± 0.1	107 ± 2	13477		6
7090	7.6	7.0	99	14130	653	7
6720	7.4 ± 0.1	6.8 ± 0.1	98 ± 1	14899	769	8

It was found that the spin splitting decreases with an increase in V_2^1 , and this is attributed to Λ losing some of its significance as the molecule vibrates with greater amplitude. Band origins were estimated for the assigned bands, and vibrational intervals were calculated. Because of some indications of Fermi resonance in the 7090 Å band, the 7410 Å and 6720 Å bands were used to obtain an estimate of the bending vibrational frequency. The estimated value is about 710 cm⁻¹. This value of v_2^1 indicates the origin of the system to be at about 9220 cm⁻¹ or 10800 Å.

The abrupt cut-off of the magnetic rotation spectrum on the violet end at low pressure at 3981 ± 3 Å is attributed to the predissociation limit corresponding to dissociation of NO₂ into NO and O, both in their ground states. Destruction

of the magnetic rotation spectrum occurs because of the onset of diffuseness. With an increase in pressure of NO_2 alone or of NO_2 plus a foreign gas the cut-off moves toward longer wave-lengths. This phenomenon is attributed to a selective pressure broadening or pressure-induced predissociation.

Recommendations.--Very few polyatomic molecules have been studied by means of their magnetic rotation spectra. In particular it is recommended that ClO_2 be studied. Apparently no one has made an attempt to observe its magnetic rotation spectrum. It is of particular interest in that it is, like NO_2 , an odd molecule. Also its absorption spectrum has been studied extensively, and Coon (56,57) has been able to make both vibrational and rotational analyses. The ground and excited states are both bent. It would be very interesting to see if a magnetic rotation spectrum exists, and if it does exist, to see how it varies with changes in field strength. An additional factor in ClO_2 is the increase in spin-orbit interaction as a result of the heavy chlorine atom. Molecules whose magnetic rotation spectra have previously been studied, such as CS_2 , might well be restudied at various field strengths with profit.

Predissociation limits are valuable in determining the dissociation energies of molecules. However, it is not always easy to find the onset of diffuseness in absorption spectra. This is particularly true if large dispersion is not available. Herzberg and Mundie (58) have suggested that at low dispersion,

diffuseness may manifest itself by apparent anomalously large intensities and may thus be identified. Magnetic rotation spectra are easily destroyed by diffuseness. It is therefore recommended that the use of magnetic rotation spectra for the detection of diffuseness and thus of predissociation limits be investigated.

APPENDIX I

ZEEMAN EFFECT IN A LINEAR TRIATOMIC MOLECULE WITH VIBRATIONAL ANGULAR MOMENTUM AND THE INTENSITY DISTRIBUTION IN THE MAGNETIC ROTATION SPECTRUM

Let us assume a linear triatomic molecule with Λ and Σ defined. In addition let us assume that quantized on the figure axis along with Λ and Σ there is angular momentum, ℓ , due to the degenerate bending mode of vibration. The magnetic moment along the figure axis is then given by the vector model of linear molecules as

$$\mu_f = (\Lambda + 2\Sigma)\mu_0 + g_n \ell \mu_n, \quad (16)$$

where μ_0 is the Bohr magneton, μ_n is the nuclear magneton, and g_n is a nuclear magnetic-gyric ratio of the order of unity and determined by the electron distribution in the molecule. However, since μ_n is small compared to μ_0 , the term in ℓ may be neglected, and the expression for μ_f reduces to

$$\mu_f = (\Lambda + 2\Sigma)\mu_0. \quad (17)$$

The component of the total angular momentum about the figure axis is equal to $\Lambda + \Sigma + \ell$. Therefore the component of magnetic moment along the total angular momentum vector is given by

$$\mu_J = \mu_f \cos(\Lambda + \Sigma + \ell, J) = \mu_f \frac{(\Lambda + \Sigma + \ell)}{\sqrt{J(J+1)}}. \quad (18)$$

The component of μ along the field direction is then given by

$$\mu_H = \mu_J \cos(H, J) = \mu_J \frac{M}{\sqrt{J(J+1)}} . \quad (19)$$

Therefore it follows that

$$\mu_H = \frac{(\Lambda + 2\Sigma)(\Lambda + \Sigma + \ell)M\mu_0}{J(J+1)} . \quad (20)$$

Displacement from the no-field position is given by $\mu_H H$. With the exception of the ℓ in the numerator the above expression for μ_H is identical with the corresponding expression for case a coupling in a diatomic molecule. The intensity distribution in the J structure of the magnetic rotation spectrum should thus be very similar to that of a diatomic molecule in case a coupling. This intensity distribution is given by Cheng (8), who shows that strong P and R branches and very weak Q branches are to be expected. Nevertheless the Zeeman splitting and thus the intensity of lines go down rapidly with increasing J. Therefore only low J values contribute significantly to the intensity, and P and R branches may not be resolved. This argument provides the justification for assuming that features represent whole subbands in the K structure in this investigation and that the feature is centered around a frequency corresponding to the band origin, i.e., very low values of J.

APPENDIX II

POLARIZATION OF TRANSITION MOMENT

Table 12 shows the character table for the point group C_{2v} , which is the point group for the bent NO_2 molecule. The symbols T and R refer to translations and rotations; for example, the symbol T_z refers to translation along the z-axis. These symbols are included in the character table to show the symmetry species to which the various translations and rotations belong. In Table 13 direct products for the point group C_{2v} are shown. Sponer and Teller (59) state:

A combination between two states is allowed if their direct product contains a term which transforms like one of the translations T_x , T_y , or T_z . The direction of this translation determines the direction of the dipole moment connected with the transition (transition moment).

In Walsh's treatment the z-axis is the figure axis (C_2) of the NO_2 molecule. The y-axis is parallel to the unique axis of the approximate, prolate symmetric top. The ground state of NO_2 is an A_1 state. Thus transitions to A_2 states are forbidden and those to A_1 , B_1 , and B_2 states are allowed with polarizations indicated by the directions of the translations given in the character table. Therefore, transitions to A_1 and B_1 states have their electric vectors vibrating perpendicular to the unique axis of the top and transitions to B_2 states parallel to the unique axis.

Table 12. Character Table for the Point Group C_{2V}

	I	$C_2(z)$	$\sigma_V(xz)$	$\sigma_V(yz)$	
A_1	+1	+1	+1	+1	T_z
A_2	+1	+1	-1	-1	R_z
B_1	+1	-1	+1	-1	T_x, R_y
B_2	+1	-1	-1	+1	T_y, R_z

The attachment of x- and y-axes to the molecule is opposite to that of Herzberg, and the definitions of B_1 and B_2 are thus interchanged.

Table 13. Direct Products for the Point Group C_{2V}

	A_1	A_2	B_1	B_2
A_1	A_1	A_2	B_1	B_2
A_2	A_2	A_1	B_2	B_1
B_1	B_1	B_2	A_1	A_2
B_2	B_2	B_1	A_2	A_1

APPENDIX III

OTHER POSSIBLE ASSIGNMENTS FOR THE TRANSITION

In the text Walsh's correlation diagram was used to interpret the assignment of the excited state of the visible system as a linear $^2\pi$ state resulting from a perpendicular transition in terms of the transition of an electron from a non-bonding orbital localized on the nitrogen atom to an anti-bonding π orbital. The effect upon bond angle and correlation with a linear π state as well as the perpendicular character of the transition were considerations in this interpretation. Intuitively it was also pleasing from the energetic standpoint. Trawick (1) has made calculations of the relative energies of the possible electronic states from considerations of overlap. He attempted to refine these calculations using the valence state ionization potentials for oxygen and nitrogen. A result of his calculations is the conclusion that a number of the non-bonding oxygen orbitals are very close to the non-bonding nitrogen orbital. Table 14 shows the possibilities for transitions from which a choice must be made, according to Trawick. Trawick's notation is used. Since he uses a different choice of x and y axes, his definitions of B_1 and B_2 are opposite to those of Walsh. Walsh's notation for B_1 and B_2 will be given

in parentheses in the direct product column.

Table 14. Possibilities for Transitions

Initial Orbital	Final Orbital	Direct Product of States	Polarization
$\psi_7(A_1, n_O)$	$\psi_{12}(B_2, \pi^*)$	$B_2(B_1)$	I
$\psi_{11}(A_2, \pi)$	$\psi_{12}(B_2, \pi^*)$	$B_1(B_2)$	II
$\psi_5(A_1, n_O)$	$\psi_{12}(B_2, \pi^*)$	$B_2(B_1)$	I
$\psi_9(A_1, n_O)$	$\psi_{12}(B_2, \pi^*)$	$B_2(B_1)$	I
$\psi_6(B_1, n_O)$	$\psi_{12}(B_2, \pi^*)$	A_2	X
$\psi_8(B_1, n_O)$	$\psi_{12}(B_2, \pi^*)$	A_2	X
$\psi_{11}(A_2, \pi)$	$\psi_4(B_1, \sigma)$	$B_2(B_1)$	I

Of these transitions only four are allowed and perpendicular. The $\psi_{11}(A_2, \pi) \rightarrow \psi_4(B_1, \sigma)$ transition is probably of much higher energy than the others. The problem is then to choose between transitions from non-bonding oxygen orbitals and the non-bonding nitrogen orbital. Trawick does this by considering the spectra of related molecules. In this investigation the sufficiency of the assigned transition to account for the magnetic rotation spectrum is coupled with the change in bond angle predicted by Walsh's diagram in arriving at a conclusion. Although it is not a necessary consequence, it is highly suggestive and correlates well with the work of others.

APPENDIX IV

SAMPLE CALCULATION OF g AND $(A''-B'')$

Consider the following features from the 7410 Å band and their assignments of $|L|$ and $|K|$:

Feature	$ L $	$ K $
6	2	0
10	4	4
12	6	6
13	0	2

Since the position of a feature relative to the zero position is given by

$$g L^2 - K^2(A''-B''),$$

the wave number interval between features 6 and 10 is given by

$$(4-16)g - (0-16)(A''-B''),$$

which leads to the equation

$$16(A''-B'') - 12g = 37 \text{ cm}^{-1}.$$

The interval 37 cm^{-1} was obtained from the spectrum (see Table 6). Similarly using features 12 and 13, the following equation is obtained:

$$-32(A''-B'') + 36g = 7.$$

Solving these two equations simultaneously yields the values

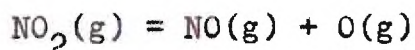
$$(A''-B'') = 7.4; g = 6.8.$$

In this way the values of g and $(A''-B'')$ were obtained, which when averaged resulted in the values given in Chapter VI and Table 11.

APPENDIX V

THERMODYNAMIC CALCULATIONS AND THE PREDISSOCIATION LIMIT

4000 Å has been assigned as the predissociation limit corresponding to the dissociation of NO_2 into NO and O, both in their ground states (43). In Chapter VI the abrupt cut-off of the magnetic rotation spectrum on the violet end at low pressure has been interpreted as due to the onset of diffuseness at this limit. It is interesting to compare the energy corresponding to the cut-off point with the results of thermodynamic calculations. From National Bureau of Standard tables the values of ΔH_f^0 at 0°K for $\text{NO}_2(\text{g})$, $\text{NO}(\text{g})$, and $\text{O}(\text{g})(^3\text{P}_2)$ were found to be 8.682, 21.477, and 58.586 kcal per mole respectively. Using these values the ΔH_0^0 for the reaction



was calculated to be 71.381 kcal per mole. Table 15 compares this result with the limit found in this investigation.

There is a difference of 141 cm^{-1} between these two values. It should be mentioned that there is a possibility that the predissociation may result in a $^2\pi_2^3$ NO state, since this state is 121.1 cm^{-1} higher than the $^2\pi_2^1$ ground state. It may also be possible that a $^3\text{P}_1$ or $^3\text{P}_2$ oxygen may result.

These states are 158 cm^{-1} and 227 cm^{-1} above the ground $3P_0$ state.

Table 15. Comparison of Cut-off and Thermodynamic Values

Units	Thermodynamic Value	Cut-off Value
Wave-length	4003 A	3981 A
Frequency	24971 cm^{-1}	25112 cm^{-1}
Kcal/mole	71.381	71.772

APPENDIX VI

TABLES

Table 16. Wave-lengths, Frequencies, and Estimated Intensities of Features from 6559 Å to 5362 Å*

Wave-length Å	Est. Intensity Scale 0-150	Frequency cm ⁻¹
6559	10	15243
6509	10	15359
6491	10	15403
6478	95	15433
6475	85	15439
6470	100	15452
6468	105	15457
6450	10	15499
6434	78	15538
6426	88	15559
6418	60	15578
6412	60	15592
6405	60	15608
6398	70	15625
6391	43	15652
6389	45	15647
6378	22	15674
6376	20	15679
6368	15	15700
6363	20	15713
6355	5	15731
6342	30	15765
6336	30	15779
6334	32	15784
6322	25	15814
6320	26	15820
6317	24	15826
6305	5	15856
6289	10	15896
6274	10	15934
6265	20	15958
6260	20	15970
6255	30	15981

*The data in Tables 16 and 17 were obtained using a slit-width of 0.5 mm and a field strength of approximately 1350 gauss.

Table 16. (Continued)

Wave-length A	Est. Intensity Scale 0-150	Frequency cm ⁻¹
6253	35	15988
6244	30	16010
6240	30	16021
6236	30	16032
6226	40	16057
6215	35	16086
6207	80	16106
6197	48	16132
6173	80	16195
6167	90	16211
6156	55	16240
6142	45	16278
6138	55	16288
6125	110	16321
6116	110	16346
6102	15	16383
6086	10	16427
6083	10	16435
6079	20	16447
6073	10	16462
6070	10	16470
6068	10	16475
6056	20	16509
6053	20	16516
6018	88	16611
6012	88	16628
6007	88	16644
5998	88	16667
5996	89	16673
5990	87	16689
5984	59	16707
5981	50	16716
5969	50	16749
5961	55	16770
5945	60	16817
5935	100	16846
5930	110	16859
5920	105	16886

Table 16. (Continued)

Wave-length A	Est. Intensity Scale 0-150	Frequency cm ⁻¹
5914	95	16904
5905	75	16930
5902	85	16938
5896	40	16955
5894	55	16963
5881	35	17000
5876	--	17015
5869	75	17035
5864	70	17050
5861	75	17057
5852	90	17083
5849	85	17093
5845	80	17103
5837	30	17128
5834	20	17137
5829	10	17151
5816	10	17190
5802	40	17232
5796	55	17248
5792	55	17262
5789	55	17270
5785	52	17282
5781	38	17293
5777	40	17305
5754	40	17376
5748	47	17393
5736	52	17430
5730	70	17448
5720	70	17477
5715	70	17495
5708	60	17514
5704	56	17527
5698	65	17545
5683	56	17591
5679	60	17603
5674	65	17618
5667	16	17641

Table 16. (Concluded)

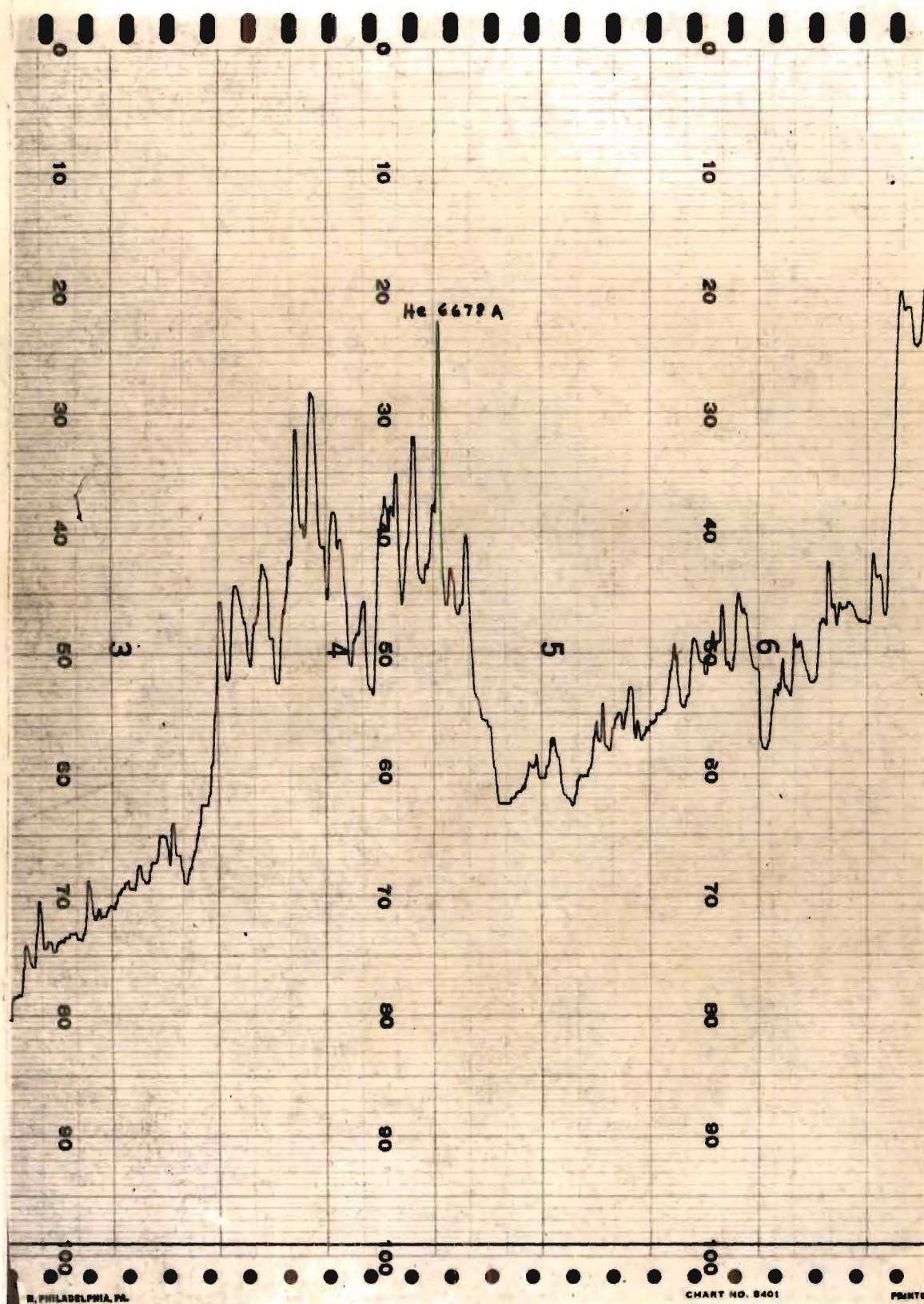
Wave-length A	Est. Intensity Scale 0-150	Frequency cm ⁻¹
5659	52	17667
5654	70	17681
5642	70	17720
5636	68	17737
5630	52	17757
5625	56	17774
5615	30	17804
5607	16	17831
5604	40	17839
5599	40	17855
5594	10	17871
5587	30	17893
5582	40	17909
5576	30	17928
5564	35	17969
5551	25	18011
5545	30	18028
5538	56	18051
5530	70	18079
5522	47	18105
5514	30	18130
5504	30	18163
5495	56	18193
5489	58	18214
5476	50	18258
5471	56	18275
5460	60	18311
5447	40	18353
5434	40	18398
5428	39	18417
5421	50	18443
5417	50	18457
5414	40	18467
5392	50	18542
5385	56	18566
5382	55	18574
5366	30	18630
5362	40	18645

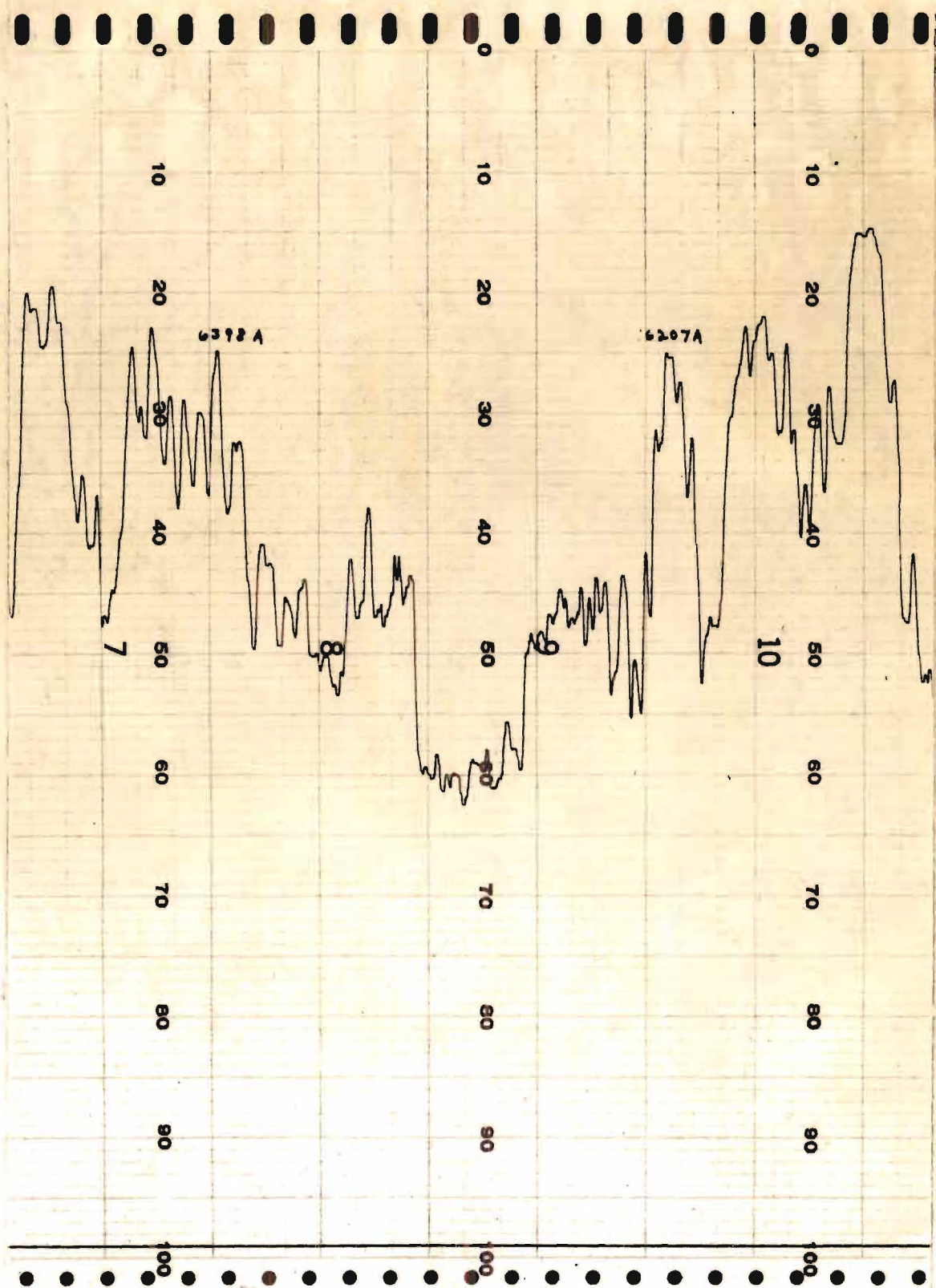
Table 17. Wave-lengths and Frequencies of Outstanding
Features from 5342 Å to 4351 Å

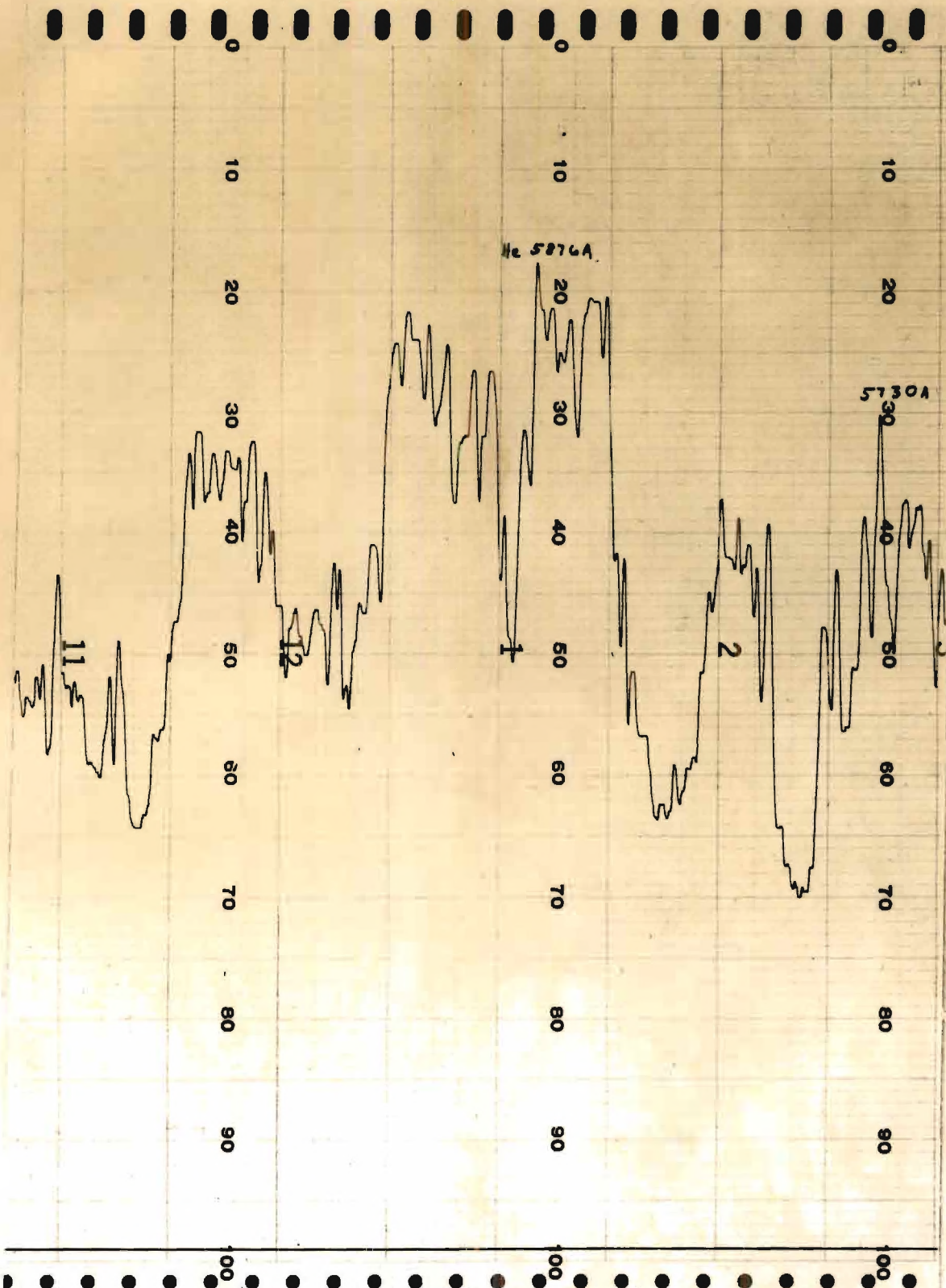
Wave-length Å	Frequency cm ⁻¹	Wave-length Å	Frequency cm ⁻¹
5342	18713	4933	20266
5326	18770	4889	20449
5303	18852	4858	20579
5290	18899	4799	20833
5277	18945	4749	21047
5264	18991	4740	21092
5261	19003	4668	21416
5254	19030	4632	21584
5250	19042	4604	21715
5231	19110	4599	21738
5205	19207	4576	21847
5199	19228	4561	21920
5184	19286	4546	21989
5124	19509	4534	22051
5112	19556	4526	22090
5098	19612	4479	22318
5066	19735	4456	22436
5051	19794	4448	22475
5029	19880	4393	22760
4951	20192	4351	22979

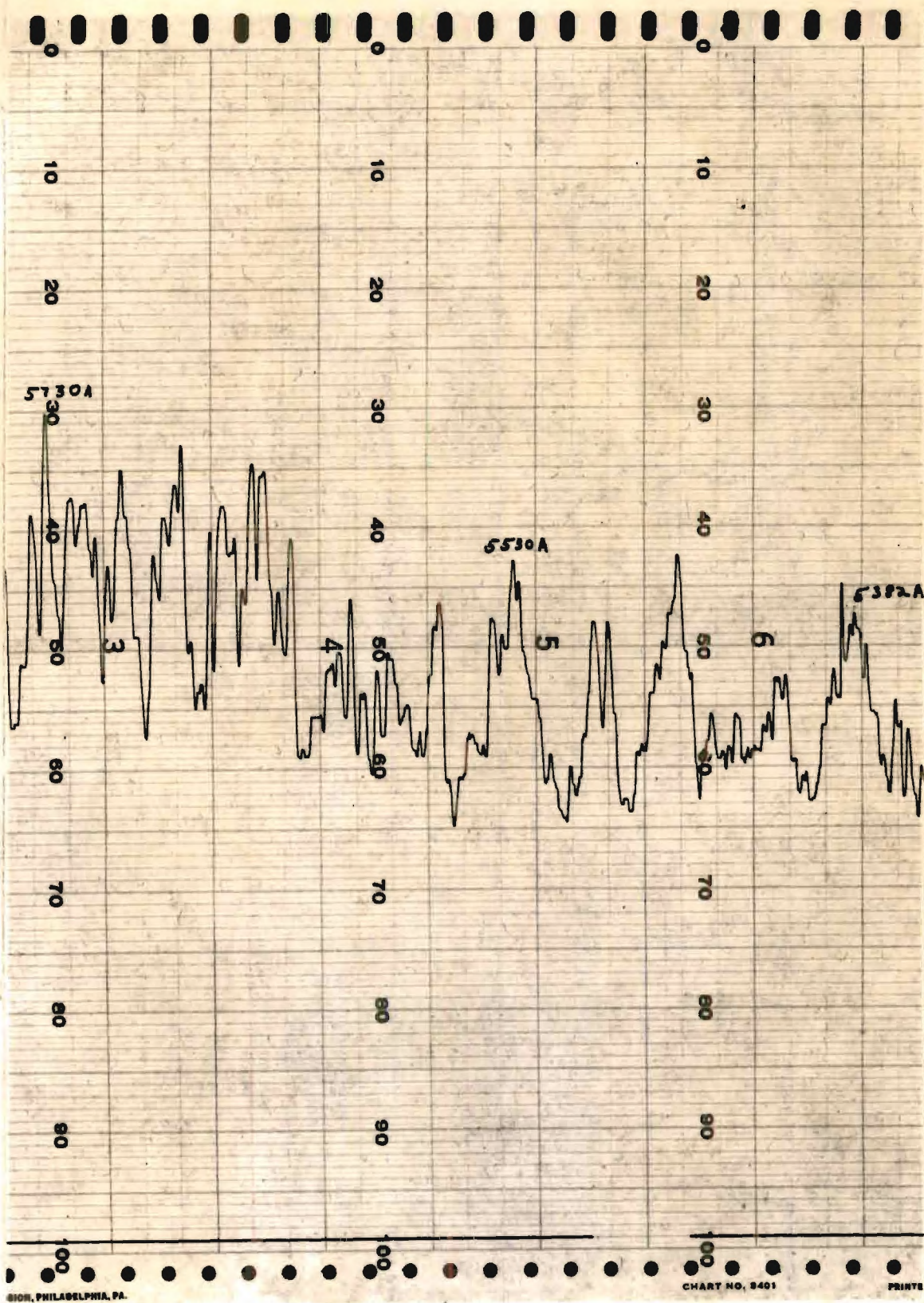
APPENDIX VII

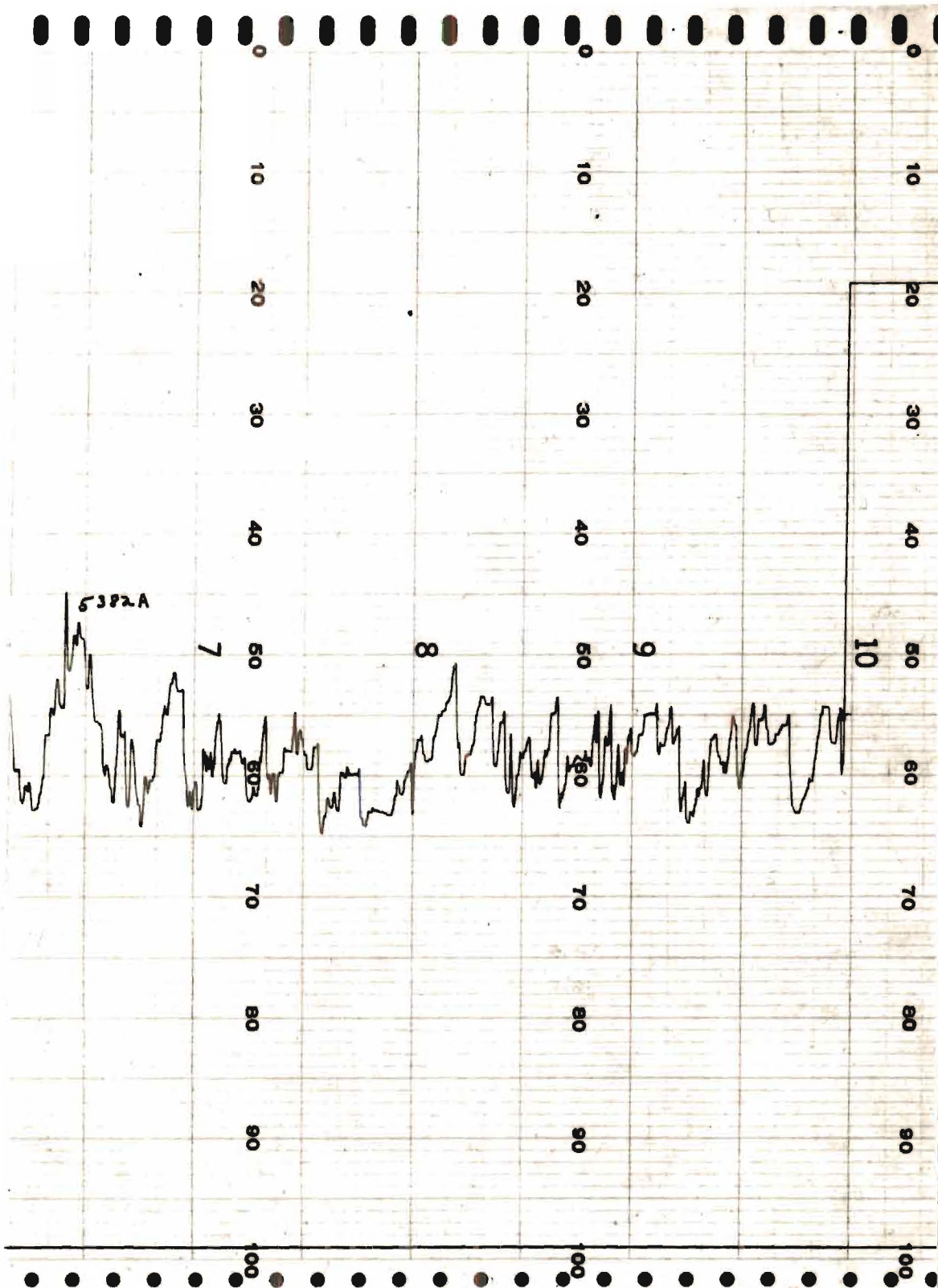
Figure 15. MICROPHOTOMETER TRACE OF THE MAGNETIC
ROTATION SPECTRUM OF NO₂ FROM 6760 Å TO 5200 Å











BIBLIOGRAPHY

1. Trawick, W. G., The Polarized Ultraviolet Absorption of Single Crystals of Polyatomic Substances at Low Temperature Unpublished Ph.D. Thesis, Georgia Institute of Technology, 1955.
2. Laidler, K. J. and K. E. Shuler, Chemical Reviews, 48, 153 (1951).
3. Loomis, F. W., Physical Review, 31, 323 (1928).
4. Loomis, F. W. and R. E. Nussbaum, Physical Review, 38, 1447 (1931).
5. Loomis, F. W. and R. E. Nussbaum, Physical Review, 39, 89 (1932).
6. Loomis, F. W. and R. E. Nussbaum, Physical Review, 40, 380 (1932).
7. Loomis, F. W. and M. J. Arvin, Physical Review, 46, 286 (1934).
8. Cheng, W., The Magnetic Rotation Spectrum of Molecules Unpublished Ph.D. Thesis, Georgia Institute of Technology, 1954.
9. Kusch, P. and F. W. Loomis, Physical Review, 55, 850 (1939).
10. Faraday, M., Philosophical Magazine, 28, 294 (1846).
11. Becquerel, H., Comptes Rendus, 125, 679 (1887).
12. Verdet, M., Annales de Chimie et de Physique, 69, 415 (1863).
13. Macaluso, D. and M. Corbino, Comptes Rendus, 127, 548 (1898).
14. Rhigi, A., Comptes Rendus, 127, 216 (1898).
15. Rhigi, A., Comptes Rendus, 128, 45 (1898).
16. Larmor, J., Aether and Matter. Cambridge: University Press, 1900.
17. Voigt, V., Annalen der Physik und Chemie (Wiedemann), 67, 345 (1899).

18. Zeeman, P., Proceedings of the Royal Academy of Sciences of Amsterdam, 5, 41 (1902).
19. Wood, R. W., Philosophical Magazine, 10, 401 (1905).
20. Fredrickson, W. R. and C. R. Stannard, Physical Review, 44, 632 (1933).
21. Wood, R. W. and G. H. Dieke, Nature, 128, 545 (1931).
22. Rosenfeld, L., Zeitschrift fur Physik, 57, 835 (1929).
23. Kronig, R. de L., Zeitschrift fur Physik, 45, 458 and 508 (1927).
24. Serber, R., Physical Review, 41, 489 (1932).
25. Carroll, T., Physical Review, 52, 822 (1937).
26. Havens, G. G., Physical Review, 41, 337 (1932).
27. Claesson, S., J. Donahue, and V. Schomaker, Journal of Chemical Physics, 16, 207 (1948).
28. Moore, G., Journal of the Optical Society of America, 43, 1045 (1953).
29. Bird, G. R., Bulletin of the American Physical Society, 30, 21 (1955).
30. McAfee, K. B., Physical Review, 78, 340 (1950).
31. McAfee, K. B., Physical Review, 82, 971 (1951).
32. Lin, Chun C., "The Spectrum of NO₂", paper presented at the Symposium on Molecular Structure and Spectroscopy, Columbus, Ohio, June 12, 1956.
33. Castle, J. G., Jr. and R. Beringer, Physical Review, 80, 114 (1950).
34. Price, W. C. and D. M. Simpson, Transactions of the Faraday Society, 37, 106 (1941).
35. Herrmann, A., Annalen der Physik, 15, 89 (1932).
36. Ionescu, A., Journal de Physique et le Radium, 8, 369 (1937).
37. Harris, L., R. W. B. Pearse, W. S. Benedict, and G. W. King, Journal of Chemical Physics, 8, 765 (1940).

38. Harris, L. and G. W. King, Journal of Chemical Physics, 8, 775 (1940).
39. Henri, V., Nature, 125, 202 (1930).
40. Curry, J. and G. Herzberg, Nature, 131, 842 (1933).
41. Dixon, J. K., Journal of Chemical Physics, 8, 157 (1940).
42. Hall, T. C. and F. E. Blacet, Journal of Chemical Physics, 20, 1745 (1952).
43. Frank, J., H. Sponer, and E. Teller, Zeitschrift fur Physikalische Chemie, B18, 88 (1932).
44. Kondratiew, V. and L. Polak, Zeitschrift fur Physik, 76, 386 (1932).
45. Norrish, R. G. W., Journal of the Chemical Society of London, 1611 (1929).
46. Neuberger, D. and A. B. F. Duncan, Journal of Chemical Physics, 22, 1693 (1954).
47. Herzberg, G., Spectra of Diatomic Molecules. New York: D. Van Nostrand Company, Inc., 1950.
48. Henderson, R. S., Physical Review, 100, 723 (1955).
49. Wilson, F. S., A Study of the Effect of Pressure on the Visible System of Ozone Unpublished Masters Thesis, Georgia Institute of Technology, 1949.
50. Kayser, H., Tabelle der Schwingungszahlen. Leipzig: S. Hirzel, 1925.
51. Ramsay, D. A., Journal of Chemical Physics, 25, 188 (1956).
52. Herzberg, G. and D. A. Ramsay, Proceedings of the Royal Society, A233, 34 (1955).
53. Mulliken, R. S., Reviews of Modern Physics, 14, 204 (1942).
54. Walsh, A. D., Journal of the Chemical Society of London, 2260 (1953).
55. Gillespie, R. J. and D. J. Millen, Quarterly Reviews, 2, 277 (1948).

- 56. Coon, J. B., Journal of Chemical Physics, 14, 665 (1946).
- 57. Coon, J. B. and E. Ortiz, A Vibrational Analysis of the 3000 - 5000 A Absorption System of ClO₂. OSR-TW-55-119. Air Research and Development Command, ²May, 1955.
- 58. Herzberg, G. and L. G. Mundie, Journal of Chemical Physics, 8, 263 (1940).
- 59. Sponer, H. and E. Teller, Reviews of Modern Physics, 13, 75 (1941).

VITA

The author was born in Dallas, Texas, on August 10, 1930, the fourth child of Isadore and Anna Goodfriend. He attended public schools in San Antonio, Texas, New Brunswick, New Jersey, and New York City. In the spring of 1948 he graduated from Granby High School in Norfolk, Virginia, and the following fall he entered the University of Virginia. He received the degree of B. S. in Chemistry from this Institution in June, 1952, at which time he was awarded the Student Medal of the American Institute of Chemists. In the fall of 1952 he entered Georgia Institute of Technology for graduate work in physical chemistry as a graduate assistant. He began work on his research under the direction of W. H. Eberhardt. On June 28, 1953, the author was married to Beverly Ann Lebar. During the summer of 1953 he was supported by money from the Research Corporation. For the 1954-55 academic year he was supported by a Departmental Fellowship awarded by the Graduate School, and from June, 1955 to June, 1956 he was a National Science Foundation Fellow. After completing his work at Georgia Tech, he accepted a post-doctoral fellowship with A. B. F. Duncan at the University of Rochester.